# Integrated mobile inventory and fleet management for an on-demand delivery system

Yang, C.; Maknoon, M. Y.; Jiang, H.; Azadeh, Sh Sharif

**DOI**
10.1016/j.trc.2025.105264

**Publication date**
2025

**Document Version**
Final published version

**Published in**
Transportation Research Part C: Emerging Technologies

Transportation Research Part C 179 (2025) 105264

Contents lists available at ScienceDirect

Transportation Research Part C

journal homepage: www.elsevier.com/locate/trc

# Integrated mobile inventory and fleet management for an on-demand delivery system

C. Yang [a], M.Y. Maknoon [b,*], H. Jiang [c], Sh. Sharif Azadeh [d]

[a] Department of Maritime and Transport Technology, Delft University of Technology, Delft, The Netherlands
[b] Engineering, Systems and Services Department, Delft University of Technology, Netherlands
[c] Department of Industrial Engineering, Tsinghua University, Beijing 100084, China
[d] Transport and Planning Department, Delft University of Technology, Netherlands

ARTICLE INFO

*Keywords:*
Meal delivery problem
Mobile fleet inventory
Capacitated facility location
Urban waterway logistics

ABSTRACT

This study introduces an optimization framework for deploying Mobile Fleet Inventories (MFIs) to address operational inefficiencies in on-demand delivery systems. Traditionally, these systems rely on stationary facilities to organize operations and manage resources. While stationary facilities provide stability and structured coverage, they are inherently rigid and struggle to adapt to the spatial and temporal fluctuations characteristic of urban service demand. By leveraging urban waterways, MFIs act as dynamic, mobile facilities, enabling real-time resource redistribution and offering greater flexibility to meet evolving demand patterns efficiently.

We formulate the problem as a mixed-integer linear programming model to optimize MFI deployment, minimizing total system costs. The model incorporates both capital investments (e.g., MFI leasing and docking infrastructure) and operational expenses (e.g., rider idle time). Key decisions include determining the optimal number, placement of MFIs, and fleet size. To validate the approach, we apply it to a meal delivery platform in Amsterdam, demonstrating its practicality and scalability. Results show that implementing MFIs reduces overall system costs by 17% and decreases rider idle time by 35% compared to stationary facility operations. These findings underscore the transformative potential of MFIs to enhance the efficiency, sustainability, and adaptability of on-demand delivery systems in urban settings.

## 1. Introduction

On-demand delivery systems have become an integral part of urban logistics, addressing the growing demand for fast and reliable deliveries in densely populated areas (Bahrami et al., 2023). These systems prioritize direct, rapid connections between vendors and customers, exemplified by meal delivery platforms that link restaurants with end-users. However, managing resource allocation and operational efficiency in these systems poses logistical challenges, particularly in dynamic urban environments.

There are two primary operational models in the meal delivery platform industry. The first is the paid-per-delivery model, where companies employ independent riders who use their personal bicycles to complete deliveries (e.g. Uber Eats). The second is the paid-per-hour model, in which companies employ riders directly and provide them with shared company-owned bikes (e.g., Just Eat Takeaway.com). This research focuses exclusively on the latter model, in which companies maintain ownership and control over delivery bikes.

* Corresponding author.
*E-mail addresses:* C.YANG@tudelft.nl (C. Yang), M.Y.Maknoon@tudelft.nl (M.Y. Maknoon), haijiang@tsinghua.edu.cn (H. Jiang), s.sharifazadeh@tudelft.nl (S.S. Azadeh).

https://doi.org/10.1016/j.trc.2025.105264
Received 25 November 2024; Received in revised form 28 June 2025; Accepted 30 June 2025
Available online 11 July 2025

A critical component of on-demand delivery systems is the micro-facility, which plays a vital role in maintaining operational efficiency. These facilities serve three primary functions: (i) housing and managing fleets of micro-delivery vehicles, such as (e)bikes and e-mopeds, (ii) redistributing delivery resources to meet the spatial and temporal variations in service demand, and (iii) serving as designated pickup and drop-off points for shift-based riders. Despite their importance, stationary facilities often fall short of meeting the dynamic and scalable requirements of on-demand services, introducing inefficiencies that limit their adaptability.

Stationary facilities provide structure and predictability in on-demand delivery systems, with each facility serving a designated coverage area. However, they struggle to adapt to fluctuating demand patterns. For example, business districts experience surges during the day, whereas residential neighborhoods see higher demand in the evening. This mismatch leads to resource imbalances: high-demand areas face shortages, while low-demand areas retain idle resources. Platforms often address these inefficiencies with truck-based redistribution or additional resources, which increase costs, contribute to congestion, and harm the environment (Du et al., 2020; DeMaio, 2009; Schuijbroek et al., 2017). Moreover, stationary facilities also present a trade-off between infrastructure investment and operational efficiency. Adding more facilities reduces idle travel, i.e., non-revenue-generating trips riders make between facilities and delivery points, but requires significant urban land and infrastructure investment. Fewer facilities lower fixed costs but worsen resource imbalances and idle travel, reducing profitability and service quality.

To address the limitations of the fixed stationary facilities, this research explores the use of electric waterborne vessels (EWVs) as Mobile Fleet Inventories (MFIs), i.e., movable facilities leveraging urban waterways to overcome the rigidity of stationary facilities. MFIs dynamically redistribute bikes to meet real-time demand while alleviating road congestion in densely populated cities. Fig. 1.1 presents a stylized illustration of the proposed MFI system. In this setup, MFIs navigate the urban canal network and riders are instructed by the platform to pick up and return bikes at docking points served by the MFIs. European initiatives, such as the canal shuttle on the Zenne (2013), warehouse ships in Paris (2016), and the parcel delivery boat Hollands Glorie in Amsterdam, demonstrate the feasibility of EWVs for urban logistics (CCNR, 2022; Parr, 2018). These projects highlight the sustainability and efficiency of EWVs, offering reduced energy consumption, increased delivery efficiency, and smaller fleet requirements.

In this paper, we introduce MFIs as a dynamic and sustainable alternative to the fixed inventory facilities in on-demand delivery systems. MFIs address key urban logistics challenges through three advantages: (i) freeing urban space by eliminating large stationary facilities, (ii) enabling bike rebalancing via underused waterways, incurring less urban noise and road congestion than using (e)trucks for rebalancing, and (iii) reducing rider idle time by streamlining bike pickup and return, thereby boosting operational efficiency.

To evaluate the feasibility and performance of MFIs, we develop a mixed-integer linear programming (MILP) model that optimizes their deployment. The model captures the trade-offs between capital investments (e.g., MFI leasing, docking location establishment, and bike acquisition) and operational costs (e.g., minimizing rider idle time). Key decisions include determining the optimal number of MFIs, selecting docking locations, and fleet sizing. This framework provides a systematic approach to designing cost-effective and efficient MFI operations.

This research makes several key contributions. First, it establishes the feasibility of the MFI system that makes use of urban waterways by demonstrating its potential to optimize overall system costs for on-demand delivery services. Second, it develops and compares two mathematical formulations: arc-based and route-based models for these systems. Third, it demonstrates the practicality and scalability of the MFI concept by adapting the model to various canal layouts and service demand scenarios. Finally, it validates the proposed approach through a case study on a meal delivery platform in Amsterdam. The results reveal that implementing MFIs can reduce overall system costs by 17% and lower average rider idle time by 35%, compared to the current usage of stationary facilities.

The remainder of this paper is organized as follows: Section 2 reviews the relevant literature, highlighting gaps and motivating the research. Section 3 formalizes the problem and defines the scope of the study. Section 4 presents the proposed mathematical formulations. Section 5 reports experimental results on generated data to test computational performance and draw managerial insights. Then we apply the model to a real-world case study in Amsterdam to showcase its practical implications. Finally, Section 6 summarizes the findings and discusses potential directions for future research.

## 2. Literature review

The problem addressed in this study involves decision-makings related to two interdependent components: the planning of MFIs, and the sizing of the delivery bike fleet stored within these MFIs. The first component is closely related to the Mobile Facility Location Problem (MFLP), which primarily focuses on the optimal placement and movement of facilities to serve clients, typically aiming to minimize total distance or cost (see Alarcon-Gerbier and Buscher (2022) and Friggstad and Salavatipour (2011)). MFLPs have been studied in a range of applications, such as healthcare (see Büsing et al. (2021) and de Vries et al. (2020)), waste collection (Alarcon-Gerbier and Buscher, 2020), and humanitarian relief (Pashapour et al., 2024; Bayraktar et al., 2022; Raghavan et al., 2019).

However, conventional MFLPs generally focus on either resource pickup (e.g., waste collection, see Alarcon-Gerbier and Buscher (2020)) or resource delivery (e.g., humanitarian relief, see Pashapour et al. (2024)), but not both. Our methodology considers both the delivery and pickup of the resources (bikes) and explicitly models inventory fluctuations over time. This constitutes our first contribution. From another perspective, the shared delivery bikes resemble an urban bike-sharing system. In typical shared-vehicle systems, storage facilities are static, and the minimum fleet size is determined under this assumption (see Çelebi et al. (2018), Hu and Liu (2016) and Qu et al. (2021)). However, this overlooks emerging opportunities where parking facilities can be mobile, which is an increasing consideration in logistics. Our model explicitly captures this mobility, considering the case where storage facilities themselves are movable. We review the relevant literature for these two topics in Sections 2.1 and 2.2, respectively.

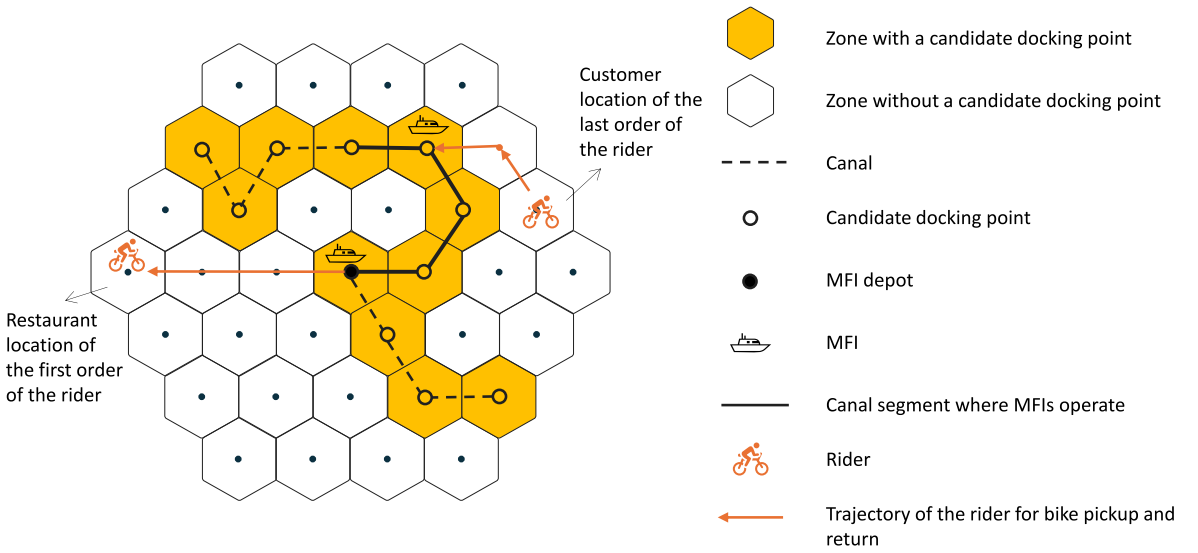


**Fig. 1.1.** An illustration of MFI system dynamics.

### 2.1. Mobile Facility Location Problem (MFLPs)

In Facility Location Problem (FLP), decisions are typically the positioning of static facilities among several candidates to serve clients through an established transportation network (Farahani and Hekmatfar, 2009). Facilities can include a variety of entities, such as transportation hubs, factories, warehouses, and fuel stations. In recent years, advances in modularization and miniaturization have led to an increase in the use of modularized mobile facilities, leading to extensive studies on related problems. The Mobile Facility Location Problem (MFLP) is first introduced by Demaine et al. (2009), which optimizes the relocation of facilities and the allocation of clients to these facilities with the aim of, for example, minimizing total transport time for both the movable facilities and the clients. Raghavan et al. (2019) further extend this problem by considering facility capacity constraints. For facilities serving as parking or storage places, like the MFI in our study, locating them close to where the resources are demanded reduces transportation distance and delivery time and helps organizations maintain low and stable inventory levels (Becker et al., 2019).

Readers are referred to Alarcon-Gerbier and Buscher (2022) for a systematic review of various topics on MFLPs. For example, Pashapour et al. (2024) examine the relocation and scheduling of mobile humanitarian facilities that are used to deliver aid service bundles to migrating refugees, with an objective to minimize total mobile facility costs. Shehadeh (2023) consider the stochastic MFLP and model the optimal sizing, routing, and scheduling of a fleet of mobile facilities. They propose two distributionally robust optimization models to study the problem and assume random demand levels in each period with unknown probability distributions. Calogiuri et al. (2021) consider the problem of relocating emergency vehicles with an objective to minimize the largest service time between assigned customers to vehicles during a multi-period planning horizon. Salman et al. (2021) consider the routing of mobile clinics to deliver healthcare to refugees. They model the problem with hierarchical objectives to minimize the number of clinics and their travel distance while maximizing refugee coverage. Yücel et al. (2020) investigate the routing of mobile medical vehicles and the selection of their stops, considering partial coverage of scored customer locations to maximize the total collected score. Alarcon-Gerbier and Buscher (2020) examine the relocation of capacitated recycling units for waste collection where the total transport time is minimized. Lei et al. (2014) study the stochastic scheduling of emergency vehicle relocation in response to traffic accidents, where uncertainties in both service demand and vehicle unavailability times are considered. Güden and Süral (2014) study an MFLP in railway construction management, synchronizing the decisions on the number, type, and schedule of capacitated mobile facilities, as well as production allocation.

### 2.2. Fleet sizing and repositioning in shared on-demand systems

In the context of shared vehicle systems, fleet sizing and repositioning have been extensively studied (see Illgen and Höck (2019), Narayanan et al. (2020) and Ataç et al. (2021)). For example, Mandal et al. (2025) consider the rider fleet sizing and scheduling problem in last-mile parcel delivery systems. They investigate the trade-off between fleet sizes and service levels, as well as the trade-off between rider shift stability and company profitability. Using extensive numerical study, they demonstrate the possibility of providing stable shifts while maintaining profitability. Fan et al. (2023) examine the strategic fleet sizing and service level design for shared autonomous vehicle systems, where operational decisions such as vehicle parking and relocation are also considered. Benjaafar et al. (2022) study the dimensioning of a shared vehicle system using a closed queueing network, where the randomness of both vehicle rental duration and vehicle availability at each location are considered in their model. Shehadeh

et al. (2021) study the regional fleet sizing problem of an on-demand last-mile transportation system, where they consider uncertain passenger demand and use stochastic programming and distributionally robust optimization to address both known and unknown demand distributions. Monteiro et al. (2021) optimize the fleet size of a car-sharing system aiming to maximize the number of customers served. They consider two service types: round-trip (pickup and drop-off locations are the same) and one-way (different pickup and drop-off locations) and conclude that round-trip service is better for scaling up.

In emerging on-demand ride-sharing systems, resource redistribution, request matching, and fleet sizing are central topics in the literature (see Chakraborty et al. (2021) and Vazifeh et al. (2018)). For instance, Auad-Perez and Van Hentenryck (2022) examine a multimodal on-demand transit system integrating bus and rail services with shared shuttle rides for last-mile connectivity. They develop a multi-objective model that jointly minimizes user travel cost and time, bus operating costs, and shuttle fleet size. Yang et al. (2023) study an electric autonomous mobility-on-demand service that incorporates endogenous congestion effects and coordinates vehicle-to-request matching, empty vehicle relocation, and charging scheduling. Using Bayesian optimization, they jointly optimize fleet size and charging infrastructure investment. Similarly, Guo et al. (2021) propose a robust optimization model to determine the minimum required fleet size in a hybrid system of autonomous and human-driven vehicles under uncertain demand. Narayan et al. (2021) analyze a hybrid on-demand service offering both private and pooled trips, where the fleet size is optimized to balance service coverage and operation efficiency.

### 2.3. Summary

To summarize, the challenges of waterborne MFIs are as follows. Urban canals are usually not fully meshed like streets. Most ground-based mobile facility models assume a fully connected road graph and use the shortest travel distance between two locations. However, canal transit can include one-way locks, narrow passages, and requirements for minimum turning radii, which prevent the application of all-pairs shortest distances on the raw canal network for all types of vessels. Moreover, the scheduling and routing of waterborne MFIs must operate within a limited number of selected docking points and align precisely with riders' dynamic shift schedules. We formulate the problem using both the arc-based and the route-based models considering these practical issues, and demonstrate the value of our approach using a realistic case study.

Our study contributes to the literature in that: (1) While mobile facility location problems (MFLPs) have been extensively studied in various applications, they typically consider unidirectional resource flows (either pickup or drop-off) and do not account for inventory fluctuations at mobile facilities. Our model departs from this by jointly modeling bike pickup and drop-off (bi-directional) operations at MFIs, with inventory levels dynamically evolving over time. (2) Research on fleet sizing in shared-vehicle systems has largely assumed static facility locations, whereas our problem considers moving parking facilities and sizes the shared delivery bike fleet accordingly. Therefore, the waterborne MFI problem extends and enriches two already challenging areas, i.e., MFLPs and shared-vehicle system fleet sizing, with both modeling and practice-relevant innovations.

## 3. Problem statement

We consider an on-demand delivery platform operating in an urban area connected by canals, such as those in Amsterdam, Leiden, or Venice. The platform utilizes two types of tools: bikes that start and end their operations from specific locations within the area, as well as electric waterborne vessels that act as MFIs.

We assume the on-demand delivery service operates under a shift-based business model, with bikes owned by the platform. Each rider shift is divided into three segments: pre-service, service, and post-service segment. During the pre-service segment, a rider picks up a bike at an MFI and rides to the first assigned meal collection station. During the service segment, the rider completes several consecutive delivery tasks. We define the duration of the service segment as between the arrival at the first meal collection station and the arrival at the last assigned customer of that shift. During the post-service time, the rider travels from the last customer to an MFI to return the bike. The combined pre- and post-service time is defined as the rider idle time, during which the rider is not actively providing delivery services.

We discretize the service area into a set of equal-sized, regular hexagon-shaped zones $z \in \mathcal{Z}$, classifying them into two groups: zones with a docking point where MFI can stop temporarily, and zones without any. This zoning system offers several advantages: equal cell area for modeling MFI movement in consistent distance units; equal distance to adjacent zones in all six directions; and the ability to easily adjust cell size for sensitivity analysis. The itineraries of MFIs include only the zones where they can dock, and we assume these zones are connected by canals, defining the operating area of MFIs. The planning horizon is divided into several equal-length periods $t \in \mathcal{T}$.

MFIs initiate their tours from a central depot with charging facilities. During their operation, MFIs selectively visit a series of docking points to load and unload bikes. Each docking point has a small staging area with limited capacity to hold bikes temporarily. MFIs must periodically return to the central depot for recharging. The routes and schedules of the MFIs must be synchronized with rider shifts to ensure all their demands for bike pickups and returns are satisfied. The objective is to minimize the total system cost, which is achieved by coordinating multiple decisions: the number of MFIs, the number and locations of docking points, the number of required bikes, and the allocation of pickup and return demands to MFIs.

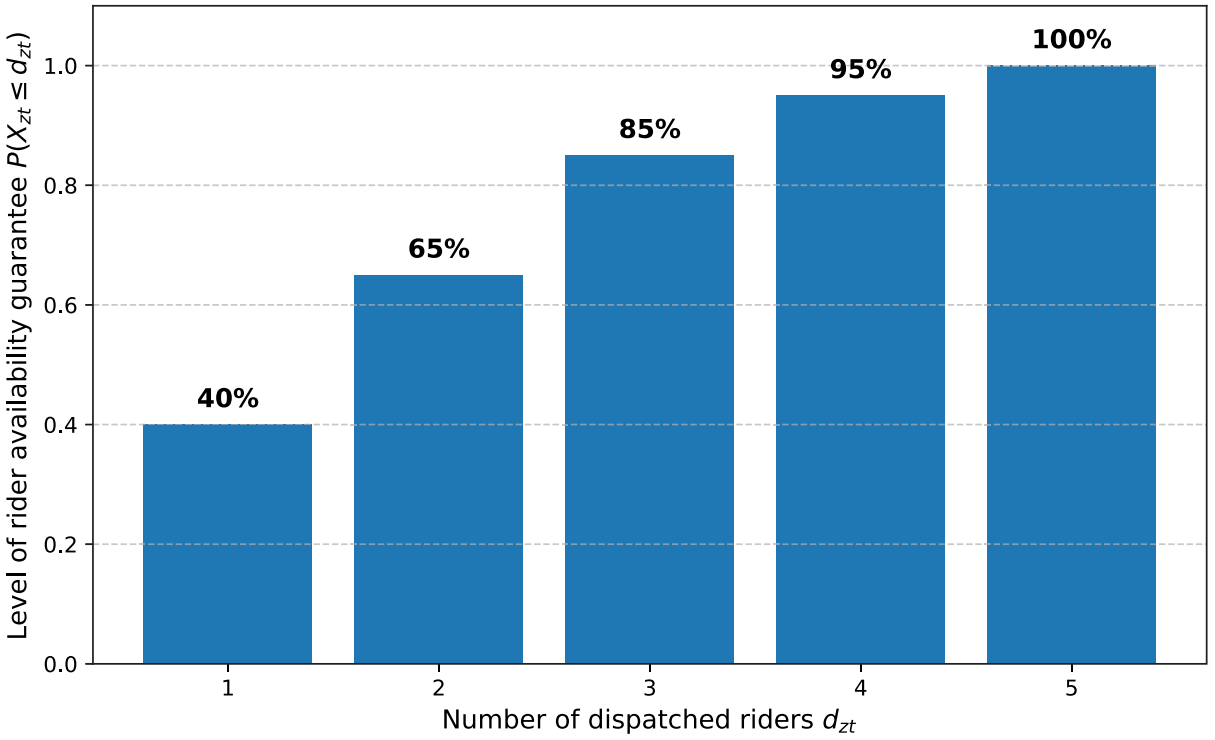


**Fig. 3.1.** Empirical cumulative probability distribution $P(X_{zt} \leq d_{zt})$ of $X_{zt}$ for a selected zone $z$ and period $t$. $X_{zt}$ is the discrete random variable representing the number of required riders, and $d_{zt}$ is the number of dispatched riders. Each bar shows the probability that the number of dispatched riders $d_{zt}$ is larger or equal to the number of required riders $X_{zt}$ based on historical data. This probability is interpreted as the level of rider availability guarantee.

### *3.1. Model bike pickup and return demands*

**Observation 1.** A rider's shift begins with a bike pickup and proceeds with a sequence of deliveries. If an MFI is located in the same zone and period as the rider's first meal collection, the bike pickup time is the shortest. Accordingly, we define the bike pickup demand as occurring in the zone and period of the first meal collection. Similarly, when the MFI is in the same zone and period as the last delivery at a customer, the bike return time is the shortest. Thus, we define the bike return demand as taking place in the zone and period of the last delivery completion. We assume MFIs are established in an existing operating area where the operator has historical information about rider itineraries.

Given the highly dynamic nature of the on-demand environment and the uncertainty of riders' first meal pickup and last delivery locations and times, we use the historical rider itinerary data to model the expected demand of bike pickups and returns as deterministic inputs. Specifically, for each zone-period pair $(z,t)$, we denote the discrete random variable $X_{zt}$ as the number of riders whose first meal collections occurred in $(z,t)$. This indicates the actual number of required riders in $(z,t)$. The value of $X_{zt}$ varies across days, its empirical distribution and the cumulative distribution function (CDF) can be estimated from historical data.

On a given planning day, the platform dispatches a predetermined number of riders to zone-period $(z,t)$, denoted $d_{zt}$. Using the empirical CDF of $X_{zt}$, we evaluate the probability $P(X_{zt} \leq d_{zt})$ that the dispatched riders suffice to meet the required number of riders. We refer to this probability as the level of rider availability guarantee, as is shown in Eq. (1).

Fig. 3.1 presents an example of the CDF of $X_{zt}$ for a specific zone-period $(z,t)$ to illustrate the level of rider availability guarantee. If $d_{zt} = 1$, then $P(X_{zt} \leq 1) = 0.4$, implying a 40% chance of satisfying the demand, i.e., a low level of rider availability guarantee. Conversely, if $d_{zt} = 5$, and $P(X_{zt} \leq 5) = 1.0$, the platform achieves full coverage of the anticipated demand. By selecting a target guarantee level, such as 80% or 100%, the platform can determine the number of riders to dispatch $(d_{zt})$. Then $d_{zt}$ is interpreted as the bike pickup demand for zone $z$ and period $t$.

$$\text{Level of rider availability guarantee} = P(d_{zt} \geq X_{zt}). \tag{1}$$

Furthermore, a transition probability $n_{zt}^{z't'}$ can be estimated from historical rider itinerary data, which indicates the probability that a rider starting the first meal collection in zone-period $(z,t)$, and will finish the last delivery in $(z',t')$. Using this transition probability, we can calculate the expected number of bike return demands in a given zone $z'$ at period $t'$, denoted as $r_{z't'}$. This is expressed as:

$$r_{z't'} = \sum_{z} \sum_{t} n_{zt}^{z't'} d_{zt}. \tag{2}$$

### 3.2. Satisfying bike pickups and returns

Riders can pick up and return bikes at an MFI, a docking point, and by self-fulfillment. Each of the three means is described as follows:

(1) **Satisfied by MFIs**. We use a set of homogeneous electric waterborne vessels $v \in \mathcal{V}$ with a fixed capacity of $Q^{MFI}$ to serve as MFIs. An MFI tour is defined as a sequence of docking point visits. The traveling time between two docking points and the duration of stay at each point are considered. An MFI can either stay at a docking point to load and unload bikes or bypass it without stopping. The MFIs start and end their tours at a central depot and must return to the depot periodically to recharge. The duration between two returns back to the depot is defined as the interval. The planning horizon is composed of several intervals, with each comprising the same number of periods. We assume the platform has real-time information on the locations of the riders and MFIs. Riders who need to pick up or return bikes will be instructed by the platform to reach a docking point to wait for the MFI. After arriving at the docking point, an MFI will wait for at least one period for riders to pick up and return bikes.

(2) **Satisfied by docking points**. The candidate locations for homogeneous docking points are assumed known. The final establishment of a docking point depends on whether it will be visited by MFIs. After a docking point is established, riders can utilize its small capacity to pick up (if available) and park bikes. We assume the platform has real-time information on the number of bikes at an established docking point. The platform can instruct riders to travel to a specific docking point for bike pickups and returns.

(3) **Self-fulfillment**. We assume the platform can direct a rider (referred to as rider A), who has finished the last delivery task, to ride to another zone where rider B, who will start the first delivery task, is instructed to wait to take over A's bike. In this case, rider B's bike pickup and rider A's return are satisfied simultaneously.

## 4. Mathematical formulation

In this section, we describe the mathematical model based on the problem description in Section 3. We introduce the graphs and sets in Section 4.1. In 4.2 we use an example to explain the satisfaction of bike pickups and returns in the spacetime network. In Sections 4.3 and 4.4 we describe the model in its arc-based and route-based formulations. The notation used in the formulations are presented in Table 4.1.

### 4.1. Network representation

We define the problem on a directed physical graph $\mathcal{G} = (\mathcal{Z}, \mathcal{E})$, where $\mathcal{Z} = \{z\}$ is the set of zones in the service area and $\mathcal{E} = \{e\}$ contains edges connecting adjacent zones in the physical graph. Each of the hexagonal zones is represented by its center and the distance between any zone and its six adjacent zones is the same, defined as a unit distance. The shortest distance between any two zones is defined as the minimum number of adjacent zone traversals required. We assume the travel distance of riders and MFIs within the same zone is zero.

The physical graph $\mathcal{G} = (\mathcal{Z}, \mathcal{E})$ is composed of two subgraphs: $\mathcal{G}^R = (\mathcal{Z}^R, \mathcal{E}^R)$ associated with the riders, and $\mathcal{G}^M = (\mathcal{Z}^M, \mathcal{E}^M)$ for the MFIs. The set $\mathcal{Z}^R \subseteq \mathcal{Z}$ comprises the zones where delivery services start and end, and $\mathcal{E}^R \subseteq \mathcal{E}$ is the subset of edges that riders can traverse. $\mathcal{Z}^M \subseteq \mathcal{Z}$ contains the zones where MFIs can be located. Specifically, an MFI located in zone $z \in \mathcal{Z}^M$ can travel through the canal to its adjacent zones, denoted by $Z^M(z)$. $\mathcal{E}^M \subseteq \mathcal{E}$ represents the set of edges that MFIs can traverse through canal connections.

The spacetime nodes (zone-period pairs) are the most fundamental concept in our model. As mentioned in Section 3, we discretize the planning horizon into a set of periods $\mathcal{T} = \{t\}$. We assume equal speed for MFIs and riders, respectively and the time for traveling one unit distance is one period. Corresponding to the physical graph $\mathcal{G}$, we define a spacetime graph $\mathcal{G}' = (\mathcal{N}, \mathcal{A})$, where $\mathcal{N} = \{(z,t) | z \in \mathcal{Z}, t \in \mathcal{T}\}$ is the set of spacetime nodes, and $\mathcal{A}$ is the set of arcs. The graph $\mathcal{G}'$ is further composed of two subgraphs: ${\mathcal{G}'}^R = (\mathcal{N}^R, \mathcal{A}^R)$ associated with riders, and ${\mathcal{G}'}^M = (\mathcal{N}^M, \mathcal{A}^M)$ for the MFIs.

In the rider associated subgraph ${\mathcal{G}'}^R = (\mathcal{N}^R, \mathcal{A}^R)$, set $\mathcal{N}^R = \mathcal{Z}^R \times \mathcal{T}$ contains spacetime nodes where riders can locate. For each node $(z,t) \in \mathcal{N}^R$, we define its successor nodes $N^{R+}_{z,t} = \{(z'',t'') | z'' \in \mathcal{Z}, t'' = t + DIS_{zz''}\}$ and predecessor nodes $N^{R-}_{z,t} = \{(z'',t'') | z'' \in \mathcal{Z}, t'' = t - DIS_{z,z''}\}$, where $DIS_{z,z''}$ is the distance between $z$ and $z''$. $\mathcal{A}^R$ is the set of rider arcs and we use $(z,t)(z'',t'')$ to represent rider movement from $z$ starting in $t$ to $z''$ arriving in $t''$. We define five rider movement types associated with the bike pickups and returns satisfaction: **PM**: pickup at MFIs and ride to first meal collections; **RM**: return to MFIs from last deliveries; **PD**: pickup at docking points and ride to first meal collections; **RD**: return to docking points from last deliveries; **SF**: self-fulfillment.

In the MFI associated subgraph ${\mathcal{G}'}^M = (\mathcal{N}^M, \mathcal{A}^M)$, set $\mathcal{N}^M$ contains spacetime nodes where MFIs can situate. For each node $(z,t)$ in $\mathcal{N}^M = \mathcal{Z}^M \times \mathcal{T}$, we define $N^{M+}_{z,t} = \{(z',t') | z' \in Z^+_z, t' = t + DIS_{zz'}\}$ as the successor nodes, and $N^{M-}_{z,t} = \{(z',t') | z' \in Z^+_z, t' = t - DIS_{zz'}\}$ as predecessor nodes. Set $\mathcal{A}^M$ comprises MFI arcs and we use $(z,t)(z',t')$ to represent MFI movement from $z$ starting in $t$ to $z'$ arriving in $t'$. Fig. 4.1 uses the spacetime node (Zone 4, Period 5) as an example to explain possible arcs associated with riders (a) and MFIs (b).

**Table 4.1**
Notation of sets, parameters, and decision variables.

| Sets | |
|---|---|
| $\mathcal{Z}$ | Set of zones, $z \in \mathcal{Z}$. |
| $\mathcal{Z}^R \subseteq \mathcal{Z}$ | Set of zones where riders start and end delivery services. |
| $\mathcal{Z}^M \subseteq \mathcal{Z}$ | Set of zones where MFIs can be located. |
| $\mathcal{T}$ | Set of discretized time periods, $t \in \mathcal{T}$. |
| $\mathcal{L}$ | Set of intervals in the planning horizon, $l \in \mathcal{L}$. |
| $\hat{T}$ | Set of interval-cut periods. |
| $\mathcal{N} = \mathcal{Z} \times \mathcal{T}$ | Set of spacetime nodes, $(z,t) \in \mathcal{N}$. |
| $\mathcal{N}^R \subseteq \mathcal{N}$ | Set of spacetime nodes associated with riders. |
| $\mathcal{N}^M \subseteq \mathcal{N}$ | Set of spacetime nodes associated with MFIs. |
| $N^{R+}_{z,t}$ | Set of successor spacetime nodes of $(z,t)$ associated with riders. |
| $N^{R-}_{z,t}$ | Set of predecessor spacetime nodes of $(z,t)$ associated with riders. |
| $N^{M+}_{z,t}$ | Set of successor spacetime nodes of $(z,t)$ associated with MFIs. |
| $N^{M-}_{z,t}$ | Set of predecessor spacetime nodes of $(z,t)$ associated with MFIs. |
| $\mathcal{A}^R$ | Set of arcs associated with riders. |
| $\mathcal{A}^M$ | Set of arcs associated with MFIs. |
| $\mathcal{V}$ | Set of MFIs, $v \in \mathcal{V}$. |
| $L$ | Set of intervals during the planning horizon, $l \in L$. |
| $\mathcal{K} = \{K_1, K_2, \ldots, K_{\lvert L \rvert}\}$ | Set of MFI route segments, $k \in \mathcal{K}$. |
| $H^{lk}$ | Set of starting nodes of holding arcs on route segment $k$ in interval $l$. |
| **Parameters** | |
| $d_{zt}$ | Number of bike pickup demands in zone $z$ period $t$ [bike]. |
| $r_{zt}$ | Number of bike return demands in zone $z$ period $t$ [bike]. |
| $Q^{MFI}$ | Capacity of homogeneous MFIs [bike]. |
| $Q^D$ | Capacity of candidate docking points [bike]. |
| $c^{MFI}$ | Daily MFI leasing cost [€/day]. |
| $c^B$ | Bike price converted to a daily rate [€/day]. |
| $c^D$ | Cost of establishing a docking point converted to a daily rate [€/day]. |
| $c^{VoT}$ | Monetary value of a period for riders [€/period]. |
| $c^{SF}$ | Cost per unit distance traveled for self-fulfillment [€/unit distance]. |
| $\lambda_{lkz} \in \{0,1\}$ | 1 if route segment k in interval l requires the candidate docking point in zone z to be established. |
| **Decision variables** | |
| $\delta^v \in \{0,1\}$ | 1 if MFI $v$ is used. |
| $x^v_{(z,t)(z',t')} \in \{0,1\}$ | 1 if MFI $v$ travels from spacetime node $(z,t)$ to $(z',t')$. |
| $\zeta_z \in \{0,1\}$ | 1 if the candidate docking point in zone $z$ is visited by MFIs. |
| $y^{PM,v}_{(z,t)(z'',t'')} \in \mathbb{Z}_{\geq 0}$ | Number of riders picking up bikes at MFI $v$ in $(z,t)$ and riding to start first delivery in $(z'',t'')$. |
| $y^{RM,v}_{(z'',t'')(z,t)} \in \mathbb{Z}_{\geq 0}$ | Number of riders returning bikes to MFI $v$ in $(z,t)$ from last delivery in $(z'',t'')$. |
| $y^{PD,v}_{(z,t)(z'',t'')} \in \mathbb{Z}_{\geq 0}$ | Number of riders picking up bikes at docking point in $(z,t)$ and riding to start first delivery in $(z'',t'')$. |
| $y^{RD,v}_{(z'',t'')(z,t)} \in \mathbb{Z}_{\geq 0}$ | Number of riders returning bikes to docking point in $(z,t)$ from last delivery in $(z'',t'')$. |
| $y^{SF}_{(z,t)(z'',t'')} \in \mathbb{Z}_{\geq 0}$ | Number of riders finishing last deliveries in $(z,t)$ and riding to $(z'',t'')$ to hand over bikes. |
| $I^v_{zt} \in \mathbb{Z}_{\geq 0}$ | Number of bikes stored in MFI $v$ at $(z,t)$. |
| $I^D_{zt} \in \mathbb{Z}_{\geq 0}$ | Number of bikes parked in docking point in $(z,t)$. |
| $\theta_{lk} \in \{0,1\}$ | 1 if the route segment $k$ in interval $l$ is in the final solution. |
| $f^{l+1,k'}_{lk} \in \{0,1\}$ | 1 if the route segment $k$ in interval $l$ and route segment $k'$ in interval $l+1$ is in the same route in the final solution. |

### 4.2. An illustrative example

In this section, we use an example to explain the satisfaction of bike pickups and returns associated with MFIs, docking points, and self-fulfillment. Consider a case where an MFI operates in a service area comprising 7 zones over a planning horizon of 10 periods, divided into 2 intervals. The canal passes sequentially through Zones 0, 6, and 5, with each zone having one candidate docking point. Some riders need to collect their first meals in Zone 4 in Period 4, and other riders will finish their last delivery task in Zone 3 in Period 7. Fig. 4.2 presents a possible allocation of these bike pickup and return demands to the MFI, docking points, or self-fulfillment. In the first interval, the MFI visits the three zones through the canal in sequence, requiring docking points in the three candidate locations to be established. In the second interval, the MFI remains stationary at the depot.

Riders who will collect their first meals in Zone 4 in Period 4 can pick up bikes: (1) at the MFI (namely **PM**): They pick up bikes at the MFI docking in Zone 5 in Period 3, then spend one period traveling to Zone 4 to start the first delivery task. (2) at a docking point (namely **PD**): They pick up bikes from the docking point in Zone 0 in Period 3, then travel to Zone 4. (3) self-fulfillment (**SF**):

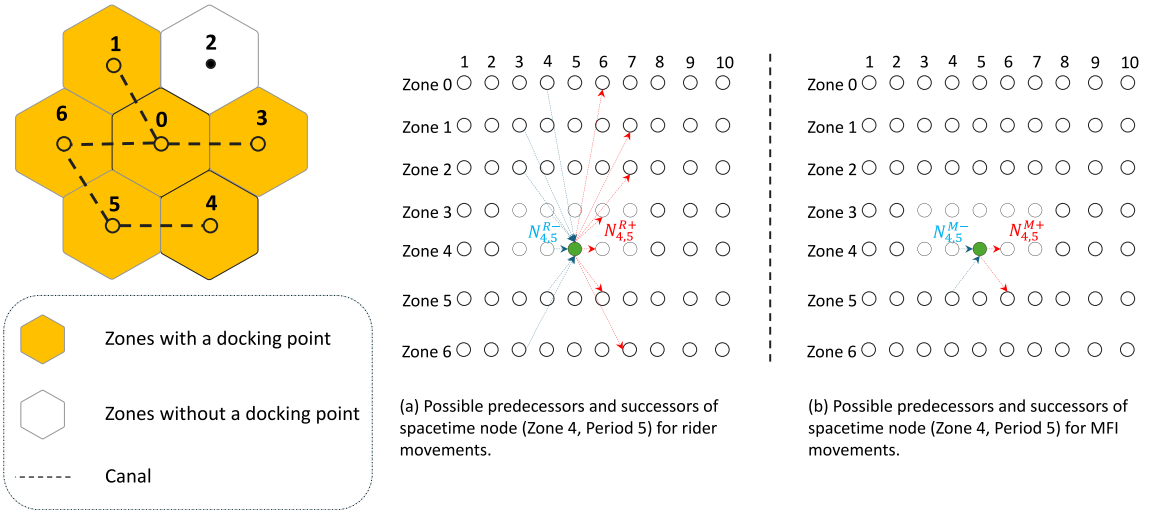


(a) Possible predecessors and successors of spacetime node (Zone 4, Period 5) for rider movements.

(b) Possible predecessors and successors of spacetime node (Zone 4, Period 5) for MFI movements.

**Fig. 4.1.** An example of arcs associated with riders (a), and with MFIs (b) for spacetime node (Zone 4, Period 5).

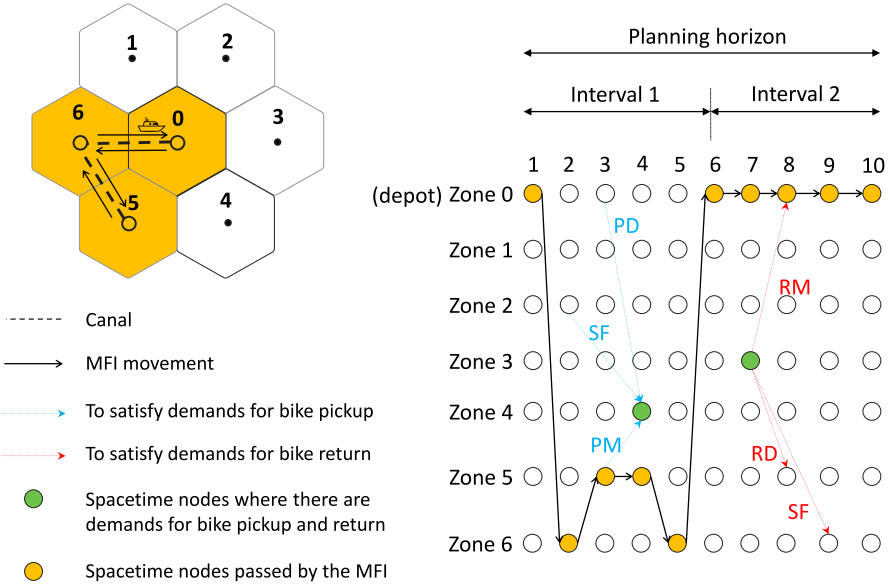


**Fig. 4.2.** An example of satisfying bikes pickup at (Zone 4, Period 4) and bikes return at (Zone 3, Period 7).

They are instructed to wait in Zone 4 for other riders who finish their last deliveries in nearby zones (e.g., Zone 2 in Period 2) to ride to their zone and hand over bikes.

Riders who complete their last deliveries in Zone 3 in Period 7 can return their bikes: (1) at the MFI (namely **RM**): They spend one period traveling to Zone 0 to return their bikes to the docked MFI. (2) at a docking point (namely **RD**): They travel to Zone 5 to park their bikes at the docking point. (3) self-fulfillment (**SF**): The platform directs them to zones (e.g., Zone 6 in Period 9) where other riders are waiting for their bikes.

### *4.3. Arc-based formulation*

We first present the families of constraints, then describe the objective function.

**MFI route constraints.** For each MFI $v \in \mathcal{V}$, we define the binary variable $\delta^v = 1$ if $v$ is deployed. Binary variable $x^v_{(z,t)(z',t')} = 1$ if MFI $v$ travels from zone $z$ to zone $z'$ starting in period $t$ arriving in period $t'$. The planning horizon is divided into a set of intervals $L = \{1, 2, \ldots, l, \ldots, |L|\}$, so that $\mathcal{T} = \{T_1, T_2, \ldots, T_l, \ldots, T_{|L|}\}$, where $|L| = \frac{|\mathcal{T}|}{|T_1|}$. We define $\tilde{T} = \{|T_1|, 2|T_1|, \ldots, l|T_1|, \ldots, (|L|-1)|T_1|\}$ as the set of periods at the end of the intervals. Constraints (3) check the usage of MFI $v$. Constraints (4) state that a used MFI must

present at the depot $z_o$ at the closure of the planning horizon. Constraints (5) ensure the MFI flow conservation at spacetime nodes. Constraints (6) make sure that no more than two MFIs stop at the same docking point in the same period except for at the depot. Constraints (7) ensure the MFIs return to the depot at the end of each interval to recharge for at least one period.

$$\delta^v = \sum_{(z',t')\in N^{M+}_{z_o,1}} x^v_{(z_o,1)(z',t')}, \quad \forall v \in \mathcal{V}, \tag{3}$$

$$\sum_{(z',t')\in N^{M+}_{z_o,1}} x^v_{(z_o,1)(z',t')} = \sum_{(z',t')\in N^{M-}_{z_o,|\mathcal{T}|}} x^v_{(z',t')(z_o,|\mathcal{T}|)}, \quad \forall v \in \mathcal{V}, \tag{4}$$

$$\sum_{(z',t')\in N^{M+}_{z,t}} x^v_{(z,t)(z',t')} = \sum_{(z',t')\in N^{M-}_{z,t}} x^v_{(z',t')(z,t)}, \quad \forall v \in \mathcal{V}, \quad \forall z \in \mathcal{Z}^M \setminus \{z_o\}, \quad \forall t \in \mathcal{T}, \tag{5}$$

$$\sum_{v\in\mathcal{V}} x^v_{(z,t)(z,t+1)} \le 1, \quad \forall z \in \mathcal{Z}^M \setminus \{z_o\}, \quad \forall t \in \mathcal{T} \setminus |\mathcal{T}|, \tag{6}$$

$$x^v_{(z_o,t)(z_o,t+1)} = 1, \quad \forall v \in \mathcal{V}, \quad \forall t \in \tilde{T}, \tag{7}$$

$$\delta^v \in \{0,1\}, \quad \forall v \in \mathcal{V}, \tag{8}$$

$$x^v_{(z,t)(z',t')} \in \{0,1\}, \quad \forall v \in \mathcal{V}, \quad \forall (z,t),(z',t') \in \mathcal{A}^M. \tag{9}$$

We let the binary variable $\zeta_z = 1$ if the candidate docking point in zone $z$ is visited by MFIs and thus is established. Constraints (10) ensure candidate docking points being visited are established. $M_1$ is a constant value set as $|\mathcal{V}|(|\mathcal{T}|-1)$.

$$\zeta_z \le \sum_{v\in\mathcal{V}} \sum_{t\in\mathcal{T}\setminus|\mathcal{T}|} x^v_{(z,t)(z,t+1)} \le M_1\zeta_z, \quad \forall z \in \mathcal{Z}^M, \tag{10}$$

$$\zeta_z \in \{0,1\}, \quad \forall z \in \mathcal{Z}^M. \tag{11}$$

**Bikes pickup and return satisfaction.** We introduce a non-negative integer variable for each of the five rider movement types described in Section 4.1, which represents bike pickups and returns at MFIs, docking point, and by self-fulfillment: $y^{PM,v}_{(z,t)(z'',t'')}$ for riders picking up bikes at MFI $v$ that is located in $z$ in period $t$ and ride to start their first delivery tasks in zone $z''$ in period $t''$; $y^{RM,v}_{(z'',t''),(z,t)}$ for riders returning bikes to MFI $v$ in $z$ in $t$ from their last deliveries in $z''$ in $t''$; $y^{PD}_{(z,t)(z'',t'')}$ for riders picking up bikes at the docking point in $z$ in period $t$ and ride to start first delivery tasks in zone $z''$ in period $t''$; $y^{RD}_{(z'',t'')(z,t)}$ for riders returning bikes to the docking point in $z$ in $t$ from the last deliveries in $z''$ in $t''$; and $y^{SF}_{(z,t)(z'',t'')}$ for riders who finish last deliveries in $z$ in $t$ and are instructed to ride to $z''$ in $t''$ to hand over bikes to other riders. As mentioned in Section 3.1, $d_{zt}$ and $r_{zt}$ are the inputs that indicate the number of the bike pickups and returns in zone $z$ in period $t$, respectively. Constraints (12) and (13) state that an MFI permits bike pickups and returns only when they are not moving. Constraints (14) and (15) ensure that a candidate docking point can allow for bike pickups and returns only if they are established. Constraints (16) (17) state that bike pickup and return demands occurring in zone $z$ in period $t$ can be satisfied by MFIs, docking points, and by self-fulfillment.

$$y^{PM,v}_{(z,t)(z'',t'')} \le d_{zt} x^v_{(z,t)(z,t+1)}, \quad \forall v \in \mathcal{V}, \quad \forall z \in \mathcal{Z}^M, \quad \forall t \in \mathcal{T} \setminus |\mathcal{T}|, \quad \forall (z'',t'') \in N^{R+}_{z,t}, \tag{12}$$

$$y^{RM,v}_{(z'',t''),(z,t)} \le r_{zt} x^v_{(z,t),(z,t+1)}, \quad \forall v \in \mathcal{V}, \quad \forall z \in \mathcal{Z}^M, \quad \forall t \in \mathcal{T} \setminus |\mathcal{T}|, \quad \forall (z'',t'') \in N^{R-}_{z,t}, \tag{13}$$

$$y^{PD}_{(z,t)(z'',t'')} \le d_{zt}\zeta_z, \quad \forall z \in \mathcal{Z}^M, \quad \forall t \in \mathcal{T}, \quad \forall (z'',t'') \in N^{R+}_{z,t}, \tag{14}$$

$$y^{RD}_{(z'',t''),(z,t)} \le r_{zt}\zeta_z, \quad \forall z \in \mathcal{Z}^M, \quad \forall t \in \mathcal{T}, \quad \forall (z'',t'') \in N^{R-}_{z,t}, \tag{15}$$

$$\sum_{v\in\mathcal{V}} \sum_{(z'',t'')\in N^{R-}_{z,t}\cap\mathcal{N}^M} y^{PM,v}_{(z'',t'')(z,t)} + \sum_{(z'',t'')\in N^{R-}_{z,t}\cap\mathcal{N}^M} y^{PD}_{(z'',t'')(z,t)} + \sum_{(z'',t'')\in N^{R-}_{z,t}} y^{SF}_{(z'',t'')(z,t)} = d_{zt}, \quad \forall (z,t) \in \mathcal{N}^R, \tag{16}$$

$$\sum_{v\in\mathcal{V}} \sum_{(z'',t'')\in N^{R+}_{z,t}\cap\mathcal{N}^M} y^{RM,v}_{(z,t)(z'',t'')} + \sum_{(z'',t'')\in N^{R+}_{z,t}\cap\mathcal{N}^M} y^{RD,v}_{(z,t)(z'',t'')} + \sum_{(z'',t'')\in N^{R+}_{z,t}} y^{SF}_{(z,t)(z'',t'')} = r_{zt}, \quad \forall (z,t) \in \mathcal{N}^R, \tag{17}$$

$$y^{PM,v}_{(z,t)(z'',t'')} \in \mathbb{Z}_{\ge 0}, \quad \forall v \in \mathcal{V}, \quad \forall z \in \mathcal{Z}^M, \quad \forall t \in \mathcal{T} \setminus |\mathcal{T}|, \quad \forall (z'',t'') \in N^{R+}_{z,t}, \tag{18}$$

$$y^{RM,v}_{(z'',t''),(z,t)} \in \mathbb{Z}_{\ge 0}, \quad \forall v \in \mathcal{V}, \quad \forall z \in \mathcal{Z}^M, \quad \forall t \in \mathcal{T} \setminus |\mathcal{T}|, \quad \forall (z'',t'') \in N^{R-}_{z,t}, \tag{19}$$

$$y^{PD}_{(z,t)(z'',t'')} \in \mathbb{Z}_{\ge 0}, \quad \forall z \in \mathcal{Z}^M, \quad \forall t \in \mathcal{T}, \quad \forall (z'',t'') \in N^{R+}_{z,t}, \tag{20}$$

$$y^{RD}_{(z'',t''),(z,t)} \in \mathbb{Z}_{\ge 0}, \quad \forall z \in \mathcal{Z}^M, \quad \forall t \in \mathcal{T}, \quad \forall (z'',t'') \in N^{R-}_{z,t}, \tag{21}$$

$$y^{SF}_{(z,t)(z'',t'')} \in \mathbb{Z}_{\ge 0}, \quad \forall (z,t)(z'',t'') \in \mathcal{A}^R. \tag{22}$$

**MFI and docking point inventory tracking.** We track the inventory of both the MFIs and docking points to ensure the capacity is not exceeded. We first discuss the MFI inventory, let non-negative integer $I^v_{zt}$ be the number of bikes stored in MFI $v$ located in zone $z$ in period $t$. If an arc $(z,t)(z',t')$ is on the spacetime route of MFI $v$, the inventory at the node $(z',t')$ equals the inventory at $(z,t)$ adding the loaded bikes and minus the unloaded ones. This is expressed in Constraints (23). Constraints (24) ensure that no inventory is considered for an MFI at a spacetime node if this node is not on the spacetime route of the MFI, and when the node is on the route the inventory will not exceed the capacity $Q^{MFI}$.

$$x^v_{(z,t)(z',t')} I^v_{z't'} = x^v_{(z,t)(z',t')} \left( I^v_{zt} + \sum_{(z'',t'')\in N^{R-}_{z,t}} y^{RM,v}_{(z'',t''),(z,t)} - \sum_{(z'',t'')\in N^{R+}_{z,t}} y^{PM,v}_{(z,t)(z'',t'')} \right),$$

$$\forall v \in \mathcal{V}, \quad \forall (z,t) \in \mathcal{N}^M, \quad \forall (z',t') \in N^{M+}_{z,t}, \tag{23}$$

$$I^v_{zt} \le \frac{Q^{MFI}}{2} \left( \sum_{(z',t')\in N^{M+}_{z,t}} x^v_{(z,t)(z',t')} + \sum_{(z',t')\in N^{M-}_{z,t}} x^v_{(z',t'),(z,t)} \right), \quad \forall v \in \mathcal{V}, \quad \forall (z,t) \in \mathcal{N}^M, \tag{24}$$

$$I^v_{zt} \in \mathbb{Z}_{\ge 0}, \quad \forall v \in \mathcal{V}, \quad \forall (z,t) \in \mathcal{N}^M. \tag{25}$$

For docking point inventories, we define the non-negative integer variable $I^D_{zt}$ as the number of bikes parked in the docking point in zone $z$ in period $t$. Similar to MFI inventories, the inventory of the docking point in $z$ in period $t$ equals the inventory in the previous period plus the bikes collected and minus the ones borrowed out, which is stated in Constraints (26). Constraints (27) ensure that the docking point inventory will never exceed the fixed capacity $Q^D$.

$$I^D_{z,t+1} = I^D_{zt} + \sum_{(z'',t'')\in N^{R-}_{z,t}} y^{RD}_{(z'',t'')(z,t)} - \sum_{(z'',t'')\in N^{R+}_{z,t}} y^{PD}_{(z,t)(z'',t'')}, \quad \forall z \in \mathcal{Z}^M, \quad \forall t \in \mathcal{T} \setminus |\mathcal{T}|, \tag{26}$$

$$I^D_{zt} \le \zeta_z Q^D, \quad \forall (z,t) \in \mathcal{N}^M, \tag{27}$$

$$I^D_{zt} \in \mathbb{Z}_{\ge 0}, \quad \forall (z,t) \in \mathcal{N}^M. \tag{28}$$

**Objective function.** The objective is to minimize the overall MFI system cost, which includes the capital investment costs that are converted to daily rates according to their usage life (MFIs leasing $J_1$, bikes purchasing $J_2$, docking points establishment $J_3$), and the opportunity costs of courier idle time spent on bike pickups and returns at MFIs and docking points $J_4$ and self-fulfillment $J_5$. Let $c^{MFI}$ represent the daily MFI leasing cost, $c^B$ the bike price converted to a daily rate, $c^D$ the cost of establishing a docking point converted to a daily rate, $c^{VoT}$ the value of a period for riders, and $c^{SF}$ the cost per unit distance traveled for self-fulfillment. The objective function is then written as:

$$MIN \quad \Phi = J_1 + J_2 + J_3 + J_4 + J_5 \tag{29}$$

where:

$$J_1 = c^{MFI} \sum_{v\in\mathcal{V}} \delta^v, \tag{30}$$

$$J_2 = c^B \Big( \sum_{v\in\mathcal{V}} I^v_{z_o,1} + \sum_{z\in\mathcal{Z}^M} I^D_{z,1} \Big), \tag{31}$$

$$J_3 = c^D \sum_{z\in\mathcal{Z}^M} \zeta_z, \tag{32}$$

$$J_4 = c^{VoT} \sum_{(z,t)\in\mathcal{N}^M} \Bigg( \sum_{(z'',t'')\in N^{R-}_{z,t}} \sum_{v\in\mathcal{V}} y^{RM,v}_{(z'',t'')(z,t)} DIS_{zz''} + \sum_{(z'',t'')\in N^{R+}_{z,t}} \sum_{v\in\mathcal{V}} y^{PM,v}_{(z,t)(z'',t'')} DIS_{zz''}$$

$$+ \sum_{(z'',t'')\in N^{R-}_{z,t}} y^{RD}_{(z'',t'')(z,t)} DIS_{zz''} + \sum_{(z'',t'')\in N^{R+}_{z,t}} y^{PD}_{(z,t)(z'',t'')} DIS_{zz''} \Bigg), \tag{33}$$

$$J_5 = c^{SF} \sum_{(z,t)(z'',t'')\in\mathcal{A}^R} y^{SF}_{(z,t)(z'',t'')} DIS_{zz''}. \tag{34}$$

### 4.4. Route-based formulation

In the arc-based formulation, each vessel movement is modeled at the arc level, enabling arc-specific constraints such as travel costs, transit times, capacity limits, and cumulative tracking (e.g., battery levels). Constraints (3)–(7) demonstrate how routing logic is implemented across arcs. This approach supports dynamic, arc-dependent constraints with pseudo-polynomial growth in decision variables and constraints, though symmetry among equivalent arc sequences may require resolution.

The route-based formulation represents each vessel route as a sequence of spacetime nodes forming a cycle over the planning horizon. Each feasible route is a single decision variable, allowing for compact modeling when the route set is manageable. Route-level constraints, e.g., duration or shift structure, are naturally enforced during generation. However, the number of routes may grow exponentially without restrictions (e.g., time windows), though practical constraints often mitigate this.

**Route selection.** As mentioned in Section 4.3, the planning horizon $\mathcal{T} = \{T_1, T_2, \dots, T_l, \dots, T_{|L|}\}$ is divided into a set of equal-length intervals. An MFI route covers the entire planning horizon, starting and ending in the depot $z_o$. During the operation, each MFI must return to depot $z_o$ at the end of every interval to recharge. This divides a route into several segments, with each segment covering one interval. Since multiple MFIs may be used, the solution can have several distinct routes, resulting in multiple route segments within an interval.

We define $\mathcal{K} = \{K_1, K_2, \dots, K_l, \dots, K_{|L|}\}$ as the set of possible MFI route segments, where $K_l$ is the set of possible route segments in interval $l$. We define the binary variable $\theta_{lk} = 1$ if route segment $k$ in interval $l$ is in the final solution. Constraints (35) and (36) ensure that there should be at least one route segment in each interval and the number of route segments in an interval should not exceed the number of available MFIs. Constraints (37) ensure that two consecutive intervals have the same number of route segments.

$$1 \le \sum_{k \in K_l} \theta_{lk}, \quad \forall l \in L, \tag{35}$$

$$\sum_{k \in K_l} \theta_{lk} \le |\mathcal{V}|, \quad \forall l \in L, \tag{36}$$

$$\sum_{k \in K_l} \theta_{lk} = \sum_{k' \in K_{l+1}} \theta_{l+1,k'}, \quad l \in L \setminus |L|, \tag{37}$$

$$\theta_{lk} \in \{0,1\}, \quad \forall l \in L, \quad \forall k \in K_l. \tag{38}$$

To decide whether two route segments in two consecutive intervals are in the same route, we define the binary variable $f_{l,k}^{l+1,k'} = 1$ if route segment $k$ in interval $l$ and route segment $k'$ in interval $l+1$ are in the same route in the solution. Constraints (39) and (40) ensure a route segment only appears in one route.

$$\theta_{lk} = \sum_{k' \in K_{l+1}} f_{l,k}^{l+1,k'}, \quad \forall l \in L \setminus \{|L|\}, \quad \forall k \in K_l, \tag{39}$$

$$\theta_{lk} = \sum_{k' \in K_{l-1}} f_{l-1,k'}^{l,k}, \quad \forall l \in L \setminus \{1\}, \quad \forall k \in K_l, \tag{40}$$

$$f_{l,k}^{l+1,k'} \in \{0,1\}, \quad \forall l \in L \setminus \{|L|\}, \quad \forall k \in K_l, \quad \forall k' \in K_{l+1}. \tag{41}$$

We define the index $\lambda_{lkz} = 1$ if route segment $k$ in interval $l$ requires the candidate docking point in zone $z$ to be established. Constraints (42) ensure if a route segment is in the solution, the corresponding candidate docking points will be established. $M_2$ is a constant value that is set as $|\mathcal{V}||L|$.

$$\zeta_z \le \sum_{l \in L} \sum_{k \in K_l} \lambda_{lkz} \theta_{lk}, \quad \forall z \in \mathcal{Z}^M, \tag{42}$$

$$\sum_{l \in L} \sum_{k \in K_l} \lambda_{lkz} \theta_{lk} \le M_2 \zeta_z, \quad \forall z \in \mathcal{Z}^M. \tag{43}$$

**Bikes pickup and return satisfaction.** MFIs can load or unload bikes only when they are stopped at docking points. In the spacetime network, this is shown by MFIs being stationed at the start of holding arcs. Let $H^{lk}$ be the set of starting nodes of holding arcs on route segment $k$ in interval $l$. We define the non-negative integer $y^{PM,lk}_{(z,t)(z'',t'')}$ indicating the number of riders who pick up bikes at MFI located at $(z,t)$ on route segment $k$ in interval $l$ and start first delivery tasks at $(z'',t'')$. Similarly, $y^{RM,lk}_{(z'',t'')(z,t)}$ represents the number of riders who return bikes to MFI at $(z,t)$ on route segment $k$ in interval $l$ after finishing last deliveries at $(z'',t'')$. Constraints (44) and (45) make sure that bikes can only be picked up from or returned to MFIs when they are docked. Similarly, bikes can only be picked up from or returned to docking points when these points are set up. This is the same as indicated in Constraints (14) and (15) in the arc-based formulation. Constraints (48) and (49) ensure the satisfaction of bike pickups and returns through MFIs, docking points, and self-fulfillment.

$$y^{PM,lk}_{(z,t)(z'',t'')} \le d_{zt} \theta_{lk}, \quad \forall l \in L, \quad \forall k \in K_l, \quad \forall (z,t) \in H^{lk}, \quad \forall (z'',t'') \in N^{R+}_{z,t}, \tag{44}$$

$$y^{RM,lk}_{(z'',t'')(z,t)} \le r_{zt} \theta_{lk}, \quad \forall l \in L, \quad \forall k \in K_l, \quad \forall (z,t) \in H^{lk}, \quad \forall (z'',t'') \in N^{R-}_{z,t}, \tag{45}$$

$$y^{PM,lk}_{(z,t)(z'',t'')} \in \mathbb{Z}_{\ge 0}, \quad \forall l \in L, \quad \forall k \in K_l, \quad \forall (z,t) \in H^{lk}, \quad \forall (z'',t'') \in N^{R+}_{z,t}, \tag{46}$$

$$y^{RM,lk}_{(z'',t'')(z,t)} \in \mathbb{Z}_{\ge 0}, \quad \forall l \in L, \quad \forall k \in K_l, \quad \forall (z,t) \in H^{lk}, \quad \forall (z'',t'') \in N^{R-}_{z,t}, \tag{47}$$

$$\sum_{l \in L} \sum_{k \in K_l} \sum_{(z'',t'') \in N^{R-}_{z,t} \cap H^{lk}} y^{PM,lk}_{(z'',t'')(z,t)} + \sum_{(z'',t'') \in N^{R-}_{z,t} \cap \mathcal{N}^M} y^{PD}_{(z'',t'')(z,t)} + \sum_{(z'',t'') \in N^{R-}_{z,t}} y^{SF}_{(z'',t'')(z,t)} = d_{zt}, \quad \forall (z,t) \in \mathcal{N}^R, \tag{48}$$

$$\sum_{l\in L}\sum_{k\in K_l}\sum_{(z'',t'')\in N^{R+}_{z,t}\cap H^{lk}} y^{RM,lk}_{(z,t)(z'',t'')} + \sum_{(z'',t'')\in N^{R+}_{z,t}\cap \mathcal{N}^M} y^{RD}_{(z,t)(z'',t'')} + \sum_{(z'',t'')\in N^{R+}_{z,t}} y^{SF}_{(z,t)(z'',t'')} = r_{zt}, \quad \forall (z,t)\in \mathcal{N}^R. \tag{49}$$

**Inventory management.** We define the non-negative integer variable $I^{lk}_{zt}$ indicating the number of bikes stored on the MFI located in $z$ in $t$ on route segment $k$ in interval $l$. The MFI capacity limit is expressed in Constraints (50).

$$I^{lk}_{zt} \le Q^{MFI}\theta_{lk}, \quad \forall l\in L, \quad \forall k\in K_l, \quad \forall (z,t)\in H^{lk}, \tag{50}$$

$$I^{lk}_{zt} \in \mathbb{Z}_{\ge 0}, \quad \forall l\in L, \quad \forall k\in K_l, \quad \forall (z,t)\in H^{lk}. \tag{51}$$

Let $H^{lk}(1)$ and $H^{lk}(-1)$ be the first and last nodes in the set $H^{lk}$. For each node $(z,t)$ in $H^{lk}$, we define $\bar{H}^{lk}_{zt}$ as its following node. Constraints (52) track the inventory update between two consecutive nodes in $H^{lk}$. Constraints (53) state that if route segment $k$ in interval $l$ and route segment $k'$ in interval $l+1$ are on the same route, the number of bikes in the MFI at the first node in $H^{l+1,k'}$ is updated based on the number at the last node in $H^{lk}$. The docking point inventory management is presented in Constraints (26) and (27).

$$I^{lk}_{\bar{H}^{lk}_{zt}} = I^{lk}_{zt} + \sum_{(z'',t'')\in N^{R-}_{z,t}} y^{RM,lk}_{(z'',t'')(z,t)} - \sum_{(z'',t'')\in N^{R+}_{z,t}} y^{PM,lk}_{(z,t)(z'',t'')}, \quad \forall l\in L, \quad \forall k\in K_l, \quad \forall (z,t)\in H^{lk}\setminus\{H^{lk}(-1)\}, \tag{52}$$

$$f^{l+1,k'}_{l,k} I^{l+1,k'}_{(z't')} = f^{l+1,k'}_{l,k}\left(I^{l,k}_{(z,t)} + \sum_{(z'',t'')\in N^{R-}_{z,t}} y^{RM,lk}_{(z'',t'')(z,t)} - \sum_{(z'',t'')\in N^{R+}_{z,t}} y^{PM,lk}_{(z,t)(z'',t'')}\right), \quad \forall l\in L\setminus\{|L|\}, \quad \forall k\in K_l, \quad \forall k'\in K_{l+1} \quad (z',t') = H^{l+1,k'}(1), \quad (z,t) = H^{lk}(-1). \tag{53}$$

**Objective function:**

$$MIN \quad \Phi' = J'_1 + J'_2 + J'_3 + J'_4 + J'_5 \tag{54}$$

where:

$$J'_1 = c^{MFI}\sum_{k\in K_1}\theta_{1k}, \tag{55}$$

$$J'_2 = c^{B}\left(\sum_{k\in K_1} I^{1,k}_{z_o,1} + \sum_{z\in\mathcal{Z}^M} I^{M}_{z,1}\right), \tag{56}$$

$$J'_3 = c^{D}\sum_{z\in\mathcal{Z}^M}\zeta_z, \tag{57}$$

$$J'_4 = c^{VoT}\left(\sum_{l\in L}\sum_{k\in K_l}\sum_{(z,t)\in H^{lk}}\left(\sum_{(z'',t'')\in N^{R-}_{z,t}} y^{RM,lk}_{(z'',t''),(z,t)} DIS_{zz''} + \sum_{(z'',t'')\in N^{R+}_{z,t}} y^{PM,lk}_{(z,t)(z'',t'')} DIS_{zz''}\right) + \sum_{(z,t)\in\mathcal{N}^M}\left(\sum_{(z'',t'')\in N^{R-}_{z,t}} y^{RD}_{(z'',t'')(z,t)} DIS_{zz''} + \sum_{(z'',t'')\in N^{R+}_{z,t}} y^{PD}_{(z,t)(z'',t'')} DIS_{zz''}\right)\right), \tag{58}$$

$$J'_5 = c^{SF}\sum_{(z,t)(z'',t'')\in\mathcal{A}^R} y^{SF}_{(z,t)(z'',t'')} DIS_{zz''}. \tag{59}$$

Some discussions are worth having here. We assume deterministic (expected) travel times for canal arcs in our model, as empirical evidence suggests that inland-waterway travel times are generally reliable and predictable. For instance, a recent study by Kruse et al. (2022) on the Upper Mississippi River reported coefficients of variation in transit times ranging from 0.2 to 1.3 across 12 segments, with most links below 0.8, indicating the low variability. Although those data do not directly come from Amsterdam, they support the broader observation that waterways tend to exhibit limited relative variability in travel times. Since our model focuses on strategic and tactical planning of MFIs, approximating travel times by their expected values is both common practice and computationally tractable.

To incorporate travel time variation and congestion, both arc-based and route-based formulations operate on a time-expanded network, where travel times between zones are defined per time period, allowing direct incorporation of time-dependent variation, i.e. routine peak-hour congestion. For more localized disruptions, such as canal closures or temporary slowdowns, the arc-based model enables arc-specific adjustments, while the route-based model can generate alternative routes to reflect changing conditions.

These features offer flexibility to model both predictable temporal patterns and localized network dynamics. Although future work may consider robust optimization, the current framework accommodates meaningful variation through deterministic, time-varying parameters aligned with strategic and tactical planning horizons.

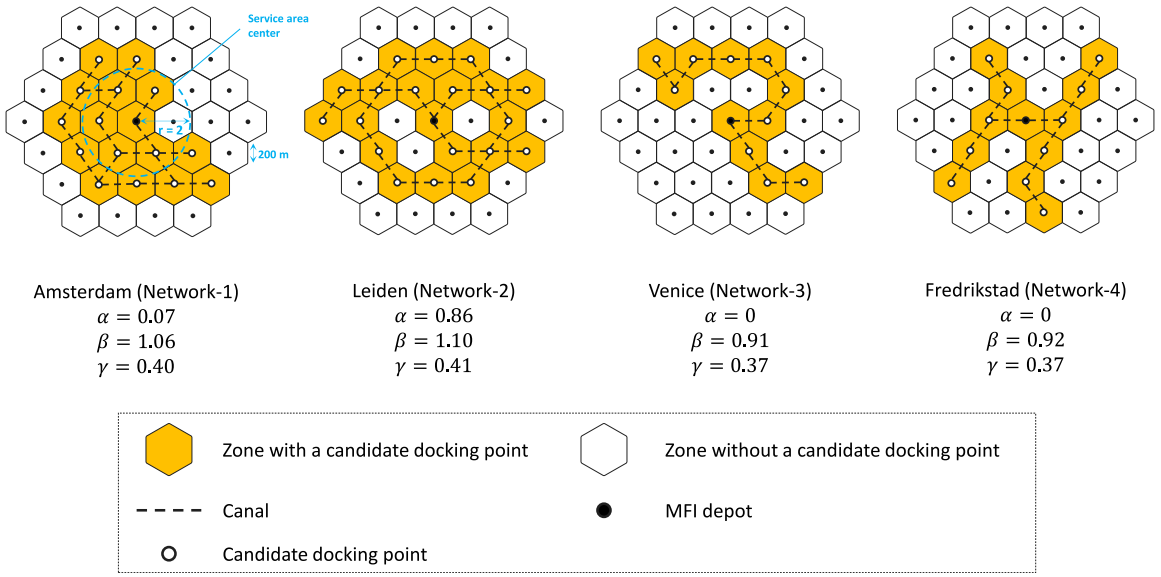


**Fig. 5.1.** Four canal network typologies replicated from Amsterdam, Leiden, Venice, and Fredrikstad.

## 5. Results

In this section, we first use the generated data to evaluate the computational performance of the model and draw managerial insights on a small scale. We then apply our framework to the Amsterdam inland waterway for a real-world case study to demonstrate the benefits of deploying MFIs. Section 5.1 details the input generation scheme; Section 5.2 compares the computational performance of the arc-based and route-based formulations; Section 5.3 presents sensitivity analyses on infrastructure configurations and operating conditions; and Section 5.4 applies the model to the Amsterdam inland waterway, evaluating platform policy effects.

### 5.1. Instance generation

We identify two service areas: an area of 37 hexagonal zones arranged in 4 circles (denoted Area-4), and an area of 91 hexagonal zones arranged in 6 circles (denoted Area-6). The edge of each zone is 200 m and one period represents 10 min. The innermost zone is chosen as the MFI depot. We further consider four canal network typologies (Fig. 5.1) that are replicated from real cities: Amsterdam (noted as Network-1), Leiden (noted as Network-1), Venice (noted as Network-1), and Fredrikstad (noted as Network-1). For each network, we calculate the following indices to indicate the complexity of the network: $\alpha$, $\beta$, and $\gamma$. The index $\alpha$ measures the degree of connectivity in a network by comparing the number of actual loops to the maximum number of circuits possible. The index $\beta$ compares the number of links to the number of nodes. The index $\gamma$ compares the number of actual links in the network to the maximum possible number of links between nodes. These indexes are calculated as:

$$\alpha = \frac{L - N + 1}{2N - 5}, \tag{60}$$

$$\beta = \frac{L}{N}, \tag{61}$$

$$\gamma = \frac{L}{3(N - 2)}. \tag{62}$$

where $L$ is the number of links, and $N$ is the number of vertices.

We consider three planning horizons: 36 periods (representing 6 h), 48 periods (representing 8 h), and 72 periods (representing 12 h). The number of active riders varies from 20 to 60 in steps of 10. Two types of spatial distribution of bike pickup and return demands are identified. In the first type (denoted as **U**), bike pickup and return demands are spatially uniformly distributed in the service area. This simulates cities without a pronounced center (e.g. Rotterdam). In the second type (denoted as **C**), 75% of the demands for bike pickup occur in the center of the area and 75% of bike returns occur in the suburbs. This mirrors cities with an obvious center like Amsterdam, where restaurants are often central and customers are usually located outside the center. The area center is defined as a circle with a radius of $r$ zones originating from the innermost zone, where $r = 2$ for Area-4 (as shown in Fig. 5.1) and $r = 3$ for Area-6. For all test cases, we consider two homogeneous MFIs available, each with a capacity $Q^{MFI}$ of 50 bikes, and the homogeneous candidate mounting points have a capacity $Q^{DP}$ of 1 bike.

In Table 5.1, we present the characteristics of the instances: (1) area size, (2) canal network typology, (3) length of the planning horizon, (4) number of riders, (5) type of spatial distribution of bike pickup and return demands. The instances are named according

**Table 5.1**
Instance characteristics.

| Characteristics | Possible choices |
|---|---|
| Area size | Area-4, Area-6 |
| Network typology | Network-1, Network-2, Network-3, Network-4 |
| Planning horizon | 36 periods, 48 periods, 72 periods |
| Number of riders | 20, 30, 40, 50, 60 |
| Type of spatial distribution of bike pickups and returns | **U**, **C** |

to the characteristics. For example, "A4-N1-P36-S40-**U**" indicates the case of Area-4, Network-1, a planning horizon of 36 periods, 40 riders, and uniformly spatially distributed bike pickups and returns.

We set the daily cost of an MFI as 810.00 €, which covers fixed costs including the MFI leasing, energy, and maintenance. The average bike price in the Netherlands is estimated at 865.00 €. We consider the service life of a new bike to be three years, so the daily cost of one bike is set as 865.00/1095.00 = 0.79 €. The Netherlands train operator NS charges about 100 € per year to store a bicycle at a train station parking lot. Based on this, we set the cost of a docking point at 100.00 € per year, that is 0.27 € per day. We consider the gross hourly salary of a rider to be 14.77 €, therefore the opportunity cost of one period of idle time of the rider is 2.46 €.

### 5.2. Computational performance

In this section, we test and compare the computational performance of the models. We conduct the experiments using Python and Gurobi Optimizer version 11.0.0. All experiments are carried out on a computer with a 2.4 GHz CPU, 8 GB of RAM, and an 8-core processor. Each instance is solved with a time limit of 4 h. In Section 5.2.1, we compare the computational performance of the arc-based and the route-based formulations. Section 5.2.2 examines the sensitivity of computation time to network typologies and geographical distribution types of bike pickup and return needs.

#### 5.2.1. Comparison between the two models

This section compares the computational performance of the arc-based and route-based formulations. We choose Network-1 and demand distribution type **U** as a representative case. We select 18 instances varying in the area size, planning horizon, and rider number (40, 60, 80). Two interval lengths are considered: 4 periods and 6 periods. We present in Table 5.2 the results of the instances with an interval length of 4 periods, and in Table 5.3 the results for the same instances with an interval length of 6 periods. The columns include the number of explored nodes (Nodes), the optimality gap (Gap), and runtime in seconds. The optimality gap is calculated as $100\times(\bar{\Phi}-LB)/\bar{\Phi}\%$, where $\bar{\Phi}$ is the best feasible solution and $LB$ is the best-known lower bound. The column "Imp" shows the improvement in solving time of the route-based model compared to the arc-based model.

It can be seen in the tables, when the numbers of riders are 40 and 60, the solution time of instances of both formulations is within one minute. However, when the number of riders reaches 80 and the planning horizon is 48 and 72 periods, neither model converges to optimality within the time limit. Table 5.4 summarizes the results from Tables 5.2 and 5.3. The results show that the route-based formulation performs better for the selected instances. Its average solution times are 4001.84 s for 4-period intervals and 4152.73 s for 6-period intervals. In contrast, the arc-based formulation takes on average 4813.84 s and 5274.22 s for the same intervals. The table also indicates that interval length affects solving time. Instances with 6-period intervals take longer to solve and have a larger optimality gap when the time limit is reached.

#### 5.2.2. Canal network and rider spatial distribution effect on computation time

In this section, we investigate the impact of canal network typology and geographical distribution of bike pickup and return needs on the solution time. We consider the four canal network typologies and the demand spatial distribution types as described in Section 5.1. We use Area-4 and planning horizon of 36 periods as a representative case and consider three rider numbers {40, 60, 80}. The selected instances are named "A4-P36-S40", "A4-P36-S60", and "A4-P36-S80". The interval length is set as 6 periods for all tests. Table 5.5 presents the computational results under different combinations of canal network typologies and demand spatial distribution types. We further summarize the results in Table 5.5 in Table 5.6. The columns include the canal network typology ("Network"), instance name, optimality gap (Gap), and solving time under demand spatial distribution type **U** and **C**.

The tables show that, on average, solving instances under canal Network-2 takes the longest time. This reflects the fact that Network-2 is the most complex network among the four networks based on the three complexity indexes described in Section 5.1. In terms of the demand spatial distributions, it takes a longer time to solve instances under spatial distribution type **C**. Specifically, solving instances with 80 riders under distribution **C** could not prove optimality within 4 h.

**Table 5.2**
Computation performance comparison of arc-based and route-based model for instances under case N1-**U** (Interval of 4 periods).

| Instance | Arc-based | | | Route-based | | | Imp. |
|---|---|---|---|---|---|---|---|
| | Nodes | Gap | Run time (s) | Nodes | Gap | Run time (s) | |
| A4-P36-S40 | 348 | 0 | 10.63 | 1 | 0 | 0.28 | 97.37% |
| A4-P36-S60 | 1 | 0 | 8.40 | 1 | 0 | 0.3 | 96.43% |
| A4-P36-S80 | 378 | 0 | 27.01 | 1 | 0 | 0.73 | 97.30% |
| A4-P48-S40 | 4496 | 0 | 11.28 | 1 | 0 | 0.97 | 91.40% |
| A4-P48-S60 | 481 | 0 | 11.97 | 1 | 0 | 0.36 | 96.99% |
| A4-P48-S80 | 1 687 422 | 1.59% | 14 400.94 | 805 144 | 0.28% | 14 402.56 | – |
| A4-P72-S40 | 11 179 | 0 | 27.21 | 1 | 0 | 0.68 | 97.50% |
| A4-P72-S60 | 5073 | 0 | 81.42 | 354 | 0 | 2.18 | 97.32% |
| A4-P72-S80 | 1 609 272 | 1.98% | 14 400.11 | 649 713 | 1.35% | 14 401.00 | – |
| A6-P36-S40 | 494 | 0 | 8.20 | 1 | 0 | 0.45 | 94.51% |
| A6-P36-S60 | 1 | 0 | 8.01 | 1 | 0 | 0.29 | 96.38% |
| A6-P36-S80 | 1 145 730 | 0.23% | 14 400.03 | 742 444 | 0.28% | 14 401.00 | – |
| A6-P48-S40 | 249 | 0 | 9.75 | 1 | 0 | 0.37 | 96.21% |
| A6-P48-S60 | 1 | 0 | 16.27 | 1 | 0 | 0.45 | 97.23% |
| A6-P48-S80 | 1 458 483 | 1.27% | 14 400.44 | 1 002 713 | 0.40% | 14 403.21 | – |
| A6-P72-S40 | 5650 | 0 | 30.48 | 41 | 0 | 0.94 | 99.99% |
| A6-P72-S60 | 4151 | 0 | 27.67 | 1 | 0 | 0.46 | 98.34% |
| A6-P72-S80 | 594 571 | 1.62% | 14 400.32 | 250 476 | 1.58% | 14 407.73 | – |

**Table 5.3**
Computation performance comparison of arc-based and route-based model for instances under case N1-**U** (Interval of 6 periods).

| Instance | Arc-based | | | Route-based | | | Imp. |
|---|---|---|---|---|---|---|---|
| | Nodes | Gap | Run time (s) | Nodes | Gap | Run time (s) | |
| A4-P36-S40 | 1727 | 0 | 25.48 | 1 | 0 | 2.75 | 89.21% |
| A4-P36-S60 | 1293 | 0 | 33.24 | 1 | 0 | 6.61 | 80.11% |
| A4-P36-S80 | 681 | 0 | 67.26 | 1 | 0 | 8.05 | 88.03% |
| A4-P48-S40 | 10 205 | 0 | 42.7 | 115 | 0 | 10.75 | 74.82% |
| A4-P48-S60 | 7386 | 0 | 92.46 | 207 | 0 | 22.53 | 75.63% |
| A4-P48-S80 | 242 860 | 1.91% | 14 400.69 | 97 615 | 1.69% | 14 400.83 | – |
| A4-P72-S40 | 148 392 | 0 | 939.19 | 9993 | 0 | 95.15 | 89.87% |
| A4-P72-S60 | 687 568 | 0.89% | 14 401.15 | 33 942 | 0 | 1283.91 | 91.08% |
| A4-P72-S80 | 314 445 | 1.97% | 14 402.54 | 272 029 | 29.10% | 14 402.13 | – |
| A6-P36-S40 | 2592 | 0 | 20.63 | 1 | 0 | 3.19 | 84.54% |
| A6-P36-S60 | 194 | 0 | 30.61 | 1 | 0 | 4.78 | 84.38% |
| A6-P36-S80 | 227 947 | 0.14% | 14 403.80 | 531 102 | 0.14% | 14 400.29 | – |
| A6-P48-S40 | 1671 | 0 | 47.58 | 1 | 0 | 6.08 | 87.22% |
| A6-P48-S60 | 2799 | 0 | 46.53 | 450 | 0 | 89.29 | −91.90% |
| A6-P48-S80 | 466 772 | 1.33% | 14 400.36 | 88 538 | 1.40% | 14 400.77 | – |
| A6-P72-S40 | 397 512 | 0 | 4181.69 | 5694 | 0 | 96.51 | 97.69% |
| A6-P72-S60 | 238 913 | 0 | 3007.53 | 4609 | 0 | 1117.97 | 62.83% |
| A6-P72-S80 | 103 437 | 26.70% | 14 401.34 | 202 307 | 5.52% | 14 402.94 | – |

**Table 5.4**
The summary of results reported in Tables 5.2 and 5.3.

| | Arc-based | | Route-based | |
|---|---|---|---|---|
| | Ave. gap | Ave. run time (s) | Ave. gap | Ave. run time (s) |
| Interval-4 periods | 0.37% | 4813.84 | 0.22% | 4001.33 |
| Interval-6 periods | 1.83% | 5274.22 | 2.10% | 4152.73 |

### *5.3. Managerial insights*

This section explores managerial insights of the MFI strategy and examines how various system characteristics affect the system performance. We use the "A4-P48-S40" instance as a representative case. This represents Area-4, with a 48-period planning horizon and 40 riders. The performance of the MFI strategy can be affected by factors both in the infrastructure and operating environment. Infrastructure factors can be canal network typologies, spatial distribution of bike pickup and return demands, MFI battery life, and the zone size and period length, which are described in Section 5.3.1. The operating environment factors involve the number of riders and the cost of self-fulfilling demand, which we present in Section 5.3.2.

#### *5.3.1. Impact of infrastructure configurations*

In this section, we identify four important infrastructure factors that can impact the performance of the MFI system: canal network typologies, spatial distribution of bike pickup and return demands, MFI battery life, and the zone size and period length.

**Table 5.5**
Computation time sensitivity to network typologies and demand spatial distribution types.

| Network | Instance | U | | C | |
|---|---|---|---|---|---|
| | | Gap | Run time (s) | Gap | Run time (s) |
| Type-1 | A4-P36-S40 | 0 | 2.67 | 0 | 8.96 |
| | A4-P36-S60 | 0 | 3.72 | 0 | 13.62 |
| | A4-P36-S80 | 0 | 2.7 | 1.54% | 14 400.13 |
| Type-2 | A4-P36-S40 | 0 | 24.61 | 0 | 12.15 |
| | A4-P36-S60 | 0 | 19.52 | 0 | 20.76 |
| | A4-P36-S80 | 0 | 29.02 | 0.62% | 14 400.44 |
| Type-3 | A4-P36-S40 | 0 | 0.82 | 0 | 1.48 |
| | A4-P36-S60 | 0 | 6.57 | 0 | 1.7 |
| | A4-P36-S80 | 0 | 1.78 | 1.44% | 14 400.08 |
| Type-4 | A4-P36-S40 | 0 | 2.21 | 0 | 11.08 |
| | A4-P36-S60 | 0 | 9.79 | 0 | 11.22 |
| | A4-P36-S80 | 0 | 14.81 | 1.44% | 14 400.10 |

**Table 5.6**
Summary of Table 5.5.

| Network | U | | C | |
|---|---|---|---|---|
| | Ave. gap | Ave. run time (s) | Ave. gap | Ave. run time (s) |
| Type-1 | 0 | 3.03 | 0.51% | 4807.47 |
| Type-2 | 0 | 24.38 | 0.21% | 4811.12 |
| Type-3 | 0 | 3.06 | 0.48% | 4801.09 |
| Type-4 | 0 | 8.94 | 0.48% | 4807.47 |

**Table 5.7**
Range of the objective values, numbers of bikes, and average idle time cross **C1**, **C2**, and **C3** for four canal network typologies under case A4-P48-S40.

| Network | Obj. (€) | Bikes | Idle (min) |
|---|---|---|---|
| 1 | [1089.83, 1159.16] | [29, 32] | [13.00, 16.38] |
| 2 | [1085.18, 1166.27] | [29, 32] | [12.75, 16.75] |
| 3 | [1087.37, 1168.19] | [29, 32] | [12.88, 16.88] |
| 4 | [1085.45, 1170.65] | [29, 32] | [12.75, 17.00] |

**Table 5.8**
Range of the objective values, numbers of bikes, and average idle time cross **U1**, **U2**, and **U3** for four canal network typologies under case A4-P48-S40.

| Network | Obj. (€) | Bikes | Idle (min) |
|---|---|---|---|
| 1 | [1149.41, 1224.00] | [27, 30] | [16.00, 19.75] |
| 2 | [1150.49, 1211.70] | [27, 30] | [16.00, 19.72] |
| 3 | [1162.25, 1245.87] | [27, 30] | [16.62, 20.88] |
| 4 | [1154.60, 1224.00] | [27, 30] | [16.25, 19.75] |

Canal network typology and demand spatial distribution. This analysis is motivated by the fact that the platform may expand its business into new cities where the canal network typology and city layout may differ. We consider the four canal network typologies and the two types of spatial distribution of bike pickup and return demands (**U** and **C**) as described in Section 5.1. For each of the two spatial distribution type, we generate three random patterns separately: {**U1**, **U2**, **U3**} and {**C1**, **C2**, **C3**}.

In Table 5.7, each row records the range of key system indicator values across the three random patterns of the **C** type of spatial distribution of bike pickups and returns for each canal network typology. Table 5.8 records the values for the **U** type for the same indicators. The "Obj. (€)" column shows the range of objective values, "Bikes" indicates the range of the numbers of bikes in the solution, and "Idle (min)" reports the range of rider idle time in minutes. The optimal solutions for all instances suggest using one MFI to serve 40 riders. As shown in the tables, for each of the canal network typology under the same type of spatial distribution of demands, three random patterns (**C1**, **C2**, **C3** for **C**; and **U1**, **U2**, **U3** for **U**) result in only slight variation in the values of the key system indicators. When comparing across the networks under the same type of spatial distribution of demands, the values of the system indicator are also close to each other. The results show that when the city layout, represented by the type of spatial distribution of demand, is fixed, the system performance of the MFI strategy under different canal network typologies and varying demand patterns remains largely consistent in terms of overall system costs and rider idle time, demonstrating the stability of the MFI strategy.

Table 5.9 compares the average value of various system indicators between the **U** and **C** type of spatial distribution of demands (Column "Distrb."). For each combination of network typology and type of spatial distribution of demands, each row records the average value of the system indicators across the three random patterns of each type of spatial distribution of demands. Under

**Table 5.9**
Comparison between **C** and **U** for four canal network typologies under case A4-P48-S40.

| Network | Distrb. | Idle (min) | Obj. (€) | Capital investment | | | Operation cost | | |
|---|---|---|---|---|---|---|---|---|---|
| | | | | Cost (€) | Bikes | DP | Cost (€) | Self-FF. (€) | Per DP (€) |
| 1 | C | 14.67 | 1123.69 | 835.05 | 30.00 | 5 | 288.64 | 22.96 | 53.14 |
| | U | 17.75 | 1183.59 | 834.27 | 28.67 | 6 | 349.32 | 18.04 | 55.21 |
| | **Diff.** | 21.00% | 5.33% | −0.09% | −4.43% | 20.00% | 21.02% | −21.43% | 3.90% |
| 2 | C | 14.71 | 1124.42 | 834.96 | 30.00 | 4.67 | 289.46 | 26.24 | 60.74 |
| | U | 17.33 | 1176.02 | 834.90 | 28.67 | 8.33 | 341.12 | 13.12 | 39.36 |
| | **Diff.** | 17.81% | 4.59% | −0.01% | −4.43% | 78.37% | 17.85% | −50.00% | −35.20% |
| 3 | C | 14.92 | 1128.25 | 834.69 | 30.00 | 3.67 | 293.56 | 31.16 | 71.56 |
| | U | 18.71 | 1202.54 | 834.36 | 28.67 | 6.33 | 368.18 | 17.22 | 55.41 |
| | **Diff.** | 25.40% | 6.58% | −0.04% | −4.43% | 72.48% | 25.42% | −44.74% | −22.57% |
| 4 | C | 14.88 | 1127.61 | 834.87 | 30.00 | 4.33 | 292.74 | 27.06 | 61.63 |
| | U | 17.92 | 1186.96 | 834.36 | 28.67 | 6.33 | 352.6 | 14.76 | 53.34 |
| | **Diff.** | 20.43% | 5.26% | −0.06% | −4.43% | 46.19% | 20.45% | −45.45% | −13.45% |

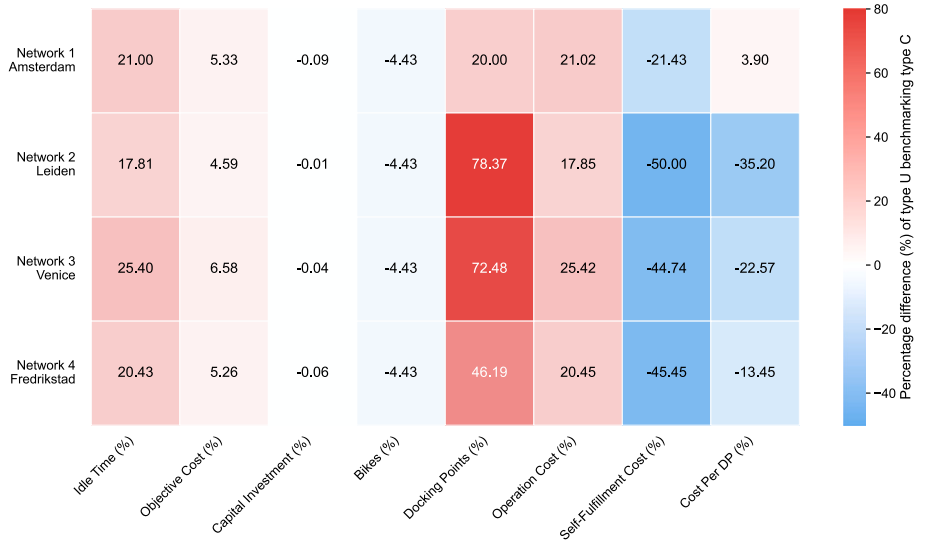


**Fig. 5.2.** A heatmap visualizing the percentage differences in the values of system indicators between **U** and **C** types of spatial distribution of bike pickup and return demands for each canal network typology.

"Capital investment", the "Cost(€)" column reports the total capital investment which is the sum of MFI leasing, bike purchasing, and docking point establishment discounted to a daily rate. The "DP" column records the number of docking points required to establish. Under "Operation cost", the "Cost(€)" column indicates the total operational cost, the "Self-FF.(€)" column shows the cost associated with self-fulfillment, and "Per DP(€)" reports the operation cost averaged to per docking point. We calculate the percentage differences in values of system indicators between **U** and **C** types of spatial distribution of bike pickup and return demands for each canal network typology in the row "Diff.", as (**U** − **C**)/**C**. The percentage differences are visualized as a heatmap in Fig. 5.2.

As shown in Table 5.9 and Fig. 5.2, under type **U**, a rider on average spends 17.81% to 25.40% more time on bike pickups and returns, and the overall system cost is approximately 5% higher. The increase in the overall system cost largely comes from the operation cost, indicating that a more spatially dispersed distribution of demands leads to an increase in the rider's idle time and the operating costs. In terms of capital investment, type **U** requires 20% to 78% more docking points but around 4% fewer bikes, resulting in a slightly lower total capital investment than in type **C**. However, for the operational costs, type **U** are about 20% higher than those of type **C**. The results suggest that platforms should carefully consider city layout when planning MFIs, as the level of demand concentration influences the riders' bike pickup and return operations and the overall system cost.

**MFI battery capacity.** The battery lifetime limits the mobility of MFIs. A longer battery lifetime allows for a longer interval between two returns of MFI to the depot during daily operation. We investigate the effect of this time interval on the system performance. For Area-4, a 0-h interval represents a stationary fleet inventory at the depot, while a 1-h interval limits MFIs to only the central zones of the service area. Intervals exceeding 2 h enable MFI to visit to outermost zones.

We use instance A4-N1-P48-S40-**U** as a representative case, which represents Area-4, Network-1, 48 periods (8 h), 40 riders and **U** type of spatial distribution of demands. We consider different intervals as {0, 1, 2, 4, 8} h. Besides the above-mentioned indicators,

**Table 5.10**
Sensitivity to the time interval between two returns of the MFI to the depot under case A4-N1-P48-S40-**U**, which represents Area-4, Network-1, 48 periods (8 h), 40 riders and **U** type of spatial distribution of demands.

| Interval (h) | Idle (min) | Obj. (€) | Capital Invest. (€) | Opr. cost (€) | Docking points | | | |
|---|---|---|---|---|---|---|---|---|
| | | | | | Nr. | Max. | Min. | Ave. |
| 0 | 19.88 | 1224.32 | 833.18 | 391.14 | 1 | 366.54 | 366.54 | 366.54 |
| 1 | 17.88 | 1185.77 | 833.99 | 351.78 | 4 | 287.82 | 4.92 | 80.56 |
| 2 | 17.50 | 1178.66 | 834.26 | 344.40 | 5 | 206.64 | 4.92 | 64.94 |
| 4 | 16.25 | 1154.33 | 834.53 | 319.80 | 6 | 91.02 | 4.92 | 51.25 |
| 8 | 16.00 | 1149.41 | 834.53 | 314.88 | 6 | 86.10 | 4.92 | 50.43 |

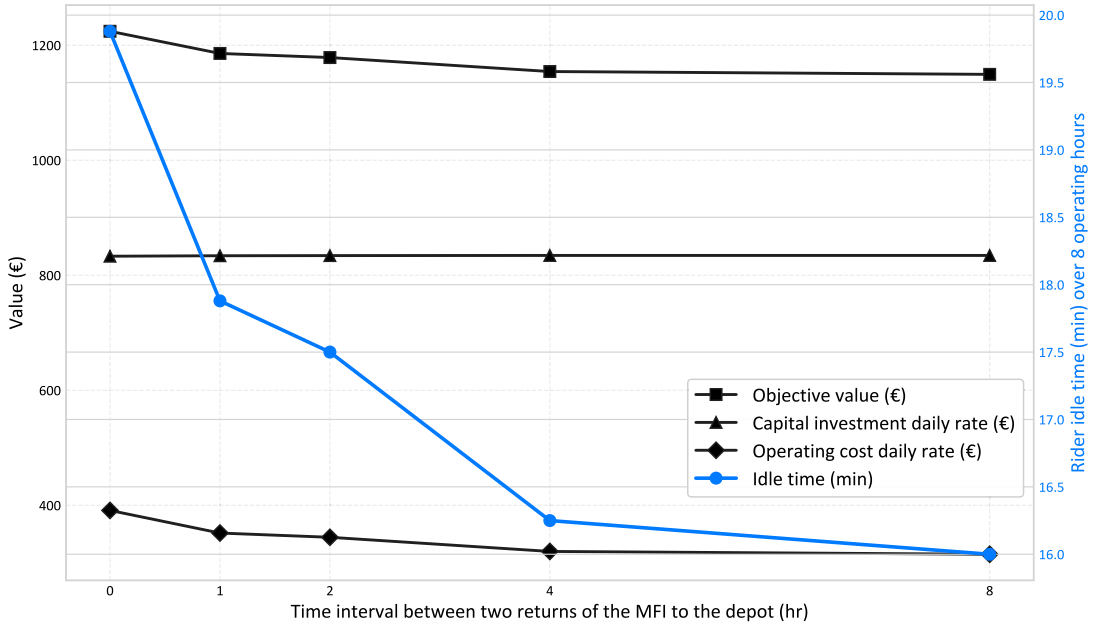


**Fig. 5.3.** Impact of the time interval between two returns of the MFI to the depot on the objective value, the capital investment converted to daily value, the daily operating cost, and the average rider idle time under case A4-N1-P48-S40-**U**, which represents Area-4, Network-1, 48 periods (8 h), 40 riders and **U** type of spatial distribution of demands.

under "Docking points" in Table 5.10, we present the number of visited docking points ("Nr.") and the maximum, minimum, and average values of the operation cost associated with the visited docking points.

As expected, more docking points are visited (from 1 to 6) as the interval increases from 0 to 8 h. However, the average rider idle time decreases from 19.88 to 16.00 min, and the objective value drops from 1224.32 € to 1149.41 € with the interval increasing. Longer interval leads to slight growth in the capital investment converted to a daily rate (from 833.18 € to 834.53 €) due to more docking points visited, but significantly reduces operation cost (from 391.14 € to 314.88 €) that is the opportunity of rider idle time. Further analysis shows that the maximum, minimum, and average values of the operation cost of the visited docking point decrease with longer interval. This is because more docking points help relieve the service burdens on each one. Furthermore, the 0-h interval scenario mimics the current static fleet inventory approach, where the highest objective value and longest average rider idle time are recorded. The results demonstrate the benefits of the MFI strategy and a higher level of MFI mobility reduces overall costs and improves rider time productivity (see Fig. 5.3).

**Zone size and period length.** This analysis examines how zone size and period length influence MFI system performance. Under the assumption of constant MFI speed, these two parameters are interdependent. The spatial resolution affects the aggregation of pickup and return demand (assumed to be located at each zone's center), the granularity of MFI movement, and model solving time.

Smaller zones increase the number of discrete areas and shorten period lengths, leading to higher model complexity and solving time. Demand becomes more spatially dispersed, necessitating more dynamic MFI routing. Conversely, coarser zoning aggregates demand and simplifies MFI movement, reducing the computational burden. The zone configuration used in other experiments reflects a trade-off between modeling precision and efficiency. We use the instance "A4-N1-P48-S40-**U**" as a reference, which represents Area-4, Network-1, 48 periods (8 h), 40 riders and **U** type of spatial distribution of demands. Three scenarios are compared: (1) Case-Base (reference): 200-m zone edge length, 10 min periods; (2) Case-Small (higher precision): 133-m zone edge length, 6.7 min periods; (3) Case-Large (lower precision): 300-m zone edge length, 15 min periods.

**Table 5.11**
Comparison of system indicators between cases with different zone-separation precisions. Case-Base uses the instance "A4-N1-P48-S40-**U**" as a reference, which represents Area-4, Network-1, 48 periods (8 h), 40 riders and **U** type of spatial distribution of demands. Case-Small considers 1.5 times shorter zone edge length. Case-Large considers 1.5 times longer zone edge length.

| Case | Obj. (€) | Cap. cost (€) | Opr. cost (€) | Idle (min) | DP | Bikes |
|---|---|---|---|---|---|---|
| Case-Base | 1185.77 | 833.99 | 351.78 | 17.88 | 4 | 29 |
| Case-Small | 1238.22 | 834.78 | 403.44 | 20.60 | 4 | 30 |
| Case-Large | 1186.90 | 832.66 | 354.24 | 18.00 | 2 | 28 |

**Table 5.12**
Sensitivity to the number of riders under case A4-N1-P48-**U**, which represents Area-4, Network-1, 48 periods, and **U** type of spatial distribution of demands.

| Rider Nr. | Obj. (€) | Cost per rider (€) | Bikes | Ratio | DP | Idle (min) |
|---|---|---|---|---|---|---|
| 20 | 984.43 | 49.22 | 16 | 0.80 | 7 | 16.25 |
| 30 | 1135.28 | 37.84 | 26 | 0.87 | 8 | 20.50 |
| 40 | 1149.41 | 28.74 | 29 | 0.73 | 6 | 16.00 |
| 50 | 1296.83 | 25.94 | 35 | 0.70 | 6 | 18.60 |
| 60 | 1403.11 | 23.39 | 46 | 0.77 | 3 | 18.83 |

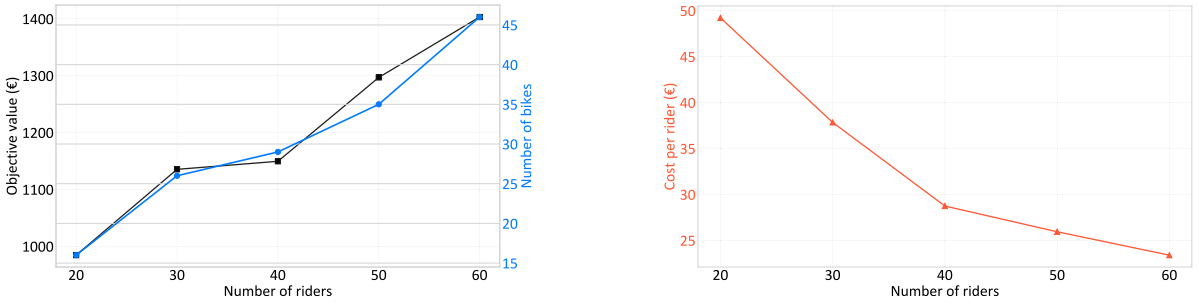


(a) Objective value and number of bikes (b) Cost per rider

**Fig. 5.4.** Effect of the number of riders on: (a) the objective value and the number of bikes required, and (b) the average cost per rider, under case A4-N1-P48-**U** which represents Area-4, Network-1, 48 periods, and **U** type of spatial distribution of demands.

Table 5.11 reports key results across the three cases, including the objective value ("Obj. (€)"), capital cost ("Cap. cost (€)"), operational cost ("Opr. cost (€)"), average idle time for pickups and returns ("Idle (min)"), number of docking points ("DP"), and number of bikes.

Case-Small yields a higher objective value, driven by increased operational cost due to more dispersed demand representation and longer rider idle times (20.60 vs. 17.88 min). In Case-Large, demand and MFI routing are more aggregated. The system becomes more static, with docking points reduced from four to two. Yet, objective value, idle time, and fleet size remain nearly unchanged relative to Case-Base. The results demonstrate the importance of spatial resolution in system design. The Case-Base configuration offers a balanced compromise—capturing essential system dynamics without excessive computational complexity or oversimplification.

### *5.3.2. Impact of operation environments*

In addition to infrastructure configurations, factors related to the operation environment are also expected to impact the planning of MFI. We identify two important characteristics: the number of riders and the unit cost of bike pickups and returns self-fulfillment.

**Sensitivity to the number of riders served**. The required number of riders in the service area highly depends on customer order volumes. We evaluate scenarios where different numbers of riders are required. We consider rider numbers as {20, 30, 40, 50, 60}, using instance A4-N1-P48-**U** as a representative case, which represents Area-4, Network-1, 48 periods, and **U** type of spatial distribution of demands.

In Table 5.12, the first column indicates the number of riders. In addition to previously discussed system indicators, we further introduce: "Cost per rider" for the total cost averaged per rider and "Ratio" for the ratio of required bikes to the number of riders. As shown in Table 5.12 and Fig. 5.4(a), as the number of riders increases from 20 to 60, the objective value rises from 984.43 € to 1403.11 € and the number of bikes grows from 16 to 46. The number of bikes maintains a ratio between 70% and 87% to the number of riders. However, as is shown in Fig. 5.4(b), the average cost per rider decreases from 49.22 € to 23.39 €. The average rider idle time fluctuates between 16 and 20.5 min. The key insight from this analysis is that the platform should carefully forecast the number of riders required and set the level of rider availability guarantee for delivery services, as it significantly influences the number of bikes required, the productivity of rider time, and overall system costs.

**Impact of unit cost for self-fulfillment** This analysis deals with situations where costs associated with bike pickup and return self-fulfillment may change. In our assumptions, the self-fulfillment is realized by considering a free-floating location in each zone

**Table 5.13**
Sensitivity to unit cost of bike pickups and returns self-fulfillment under case A4-N1-P48-**U**.

| $c^{SF}/c^{vot}$ | Obj. (€) | By MFI (%) | By DP (%) | By Self-FF. (%) | Idle (min) |
|---|---|---|---|---|---|
| 1 | 1149.41 | 72 | 20 | 7 | 16.00 |
| 1.2 | 1151.87 | 75 | 17 | 7 | 16.00 |
| 1.4 | 1153.84 | 75 | 20 | 5 | 16.12 |
| 1.6 | 1154.82 | 75 | 20 | 5 | 16.12 |
| 1.8 | 1155.81 | 72 | 22 | 5 | 16.12 |
| 2 | 1156.79 | 75 | 20 | 5 | 16.12 |
| No Self-FF. | 1159.52 | 72 | 28 | 0 | 16.5 |

**Table 5.14**
Comparison between the MFI-Base and the benchmark.

| Case | Obj. (€) | Idle (min) |
|---|---|---|
| Benchmark | 1656.13 | 37.11 |
| MFI-Base | 1373.44 | 24.11 |
| **Impr.** | 17.07% | 35.03% |

where two riders meet to hand over the bike. In some cities, this may involve additional administration costs. We increase the ratio $c^{SF}/c^{vot}$ as {1, 1.2, 1.4, 1.6, 1.8, 2} to investigate the effect of $c^{SF}$, which is the cost for one bike covering one unit distance for self-fulfillment, and $c^{vot}$ is the value of time of riders. In Table 5.13, the columns "By MFI (%)", "By DP (%)", and "By Self-FF. (%)" indicate the proportion of bike pickups and returns satisfied by the MFI, docking points, and self-fulfillment, respectively. The results show that the objective value slightly increases from 1149.41 € to 1156.79 € with the growing $c^{SF}$. Bike pickups and returns that are satisfied by self-fulfillment decrease from 7% to 5% after $c^{SF}$ increases. The average ride idle time also slightly increases, from 16.00 min to 16.12 min.

We further introduce the case where self-fulfillment is not allowed in the service area. The values of the corresponding indicators are recorded in row "No Self-FF.". We compare the case of no self-fulfillment to the case of $c^{SF}/c^{vot} = 1$. There is an increase of 0.88% in the objective value and 3.13% in the average rider idle time after shutting down self-fulfillment. The results indicate the benefits of introducing self-fulfillment to the MFI system based on overall costs and rider time productivity.

### *5.4. Case study on amsterdam inland waterway*

In this section, we apply our model to data collected from a local meal delivery platform in Amsterdam, The Netherlands. We use rider itinerary recordings in inland waterway between September 13, 2021, and October 10, 2021 as our sample. We manually outline the canal course for the gridded service area, which contains 91 zones (Fig. 5.5). The actual canal is seen as in Fig. 5.6 (right). Each zone has an edge length of 200 m, and the distance between the centers of two adjacent zones is 347 m. We consider one available MFI with a capacity of 50 bikes (see Fig. 5.6 left). We assume all zones crossed by canals can establish a docking point. Given the curved canals and the busy waterway transport on the canal, we consider a speed of 4 km/h for the MFI. For the chosen area, we select the innermost zone as the depot. The MFI is required to return to the depot every 8 h to recharge.

We consider the operation of a typical day from 9:00 to 24:00. The data indicates that the highest density of meal pickups and drop-offs occur in the canal area and they are almost spatially uniformly distributed. After averaging the monthly rider schedules to one day and removing riders that operate outside the chosen area, we obtained an average of 45 riders in a day for the canal area. The lunch peak for rider fleet dispatching is in the hour of 11:00, and the dinner peak is in the hours of 16:00 and 17:00. The parameters related to the capital investments and MFI operations are the same as described in Section 5.1.

In Section 5.4.1, we compare the MFI strategy against the static fleet inventory approach that is used in the current practice. In Section 5.4.2, we consider the day of the week to show the stability of the MFI strategy. Section 5.4.3 investigates the effects of platform policies on the service time and spatial range of the rider shift.

#### *5.4.1. Benchmarking again static fleet inventory*

We first define the base case of the MFI strategy that considers the average daily number of riders, which is 45, and name it "MFI-Base". We further construct a benchmark that mimics the static fleet inventory approach currently used by the platform. We solve the model to an optimality gap of 3%.

In Table 5.14, row "Impr." presents the percentage difference between the indicator values of MFI-Base and the benchmark. The solutions suggest both the MFI-Base and benchmark require 31 bikes for the 45 riders to conduct services. As can be seen from the table, there is a 17.07% saving in the overall system costs and a 35.03% reduction in the average rider idle time after applying the MFI strategy, which demonstrates the benefits of the strategy based on the system cost and rider time productivity.

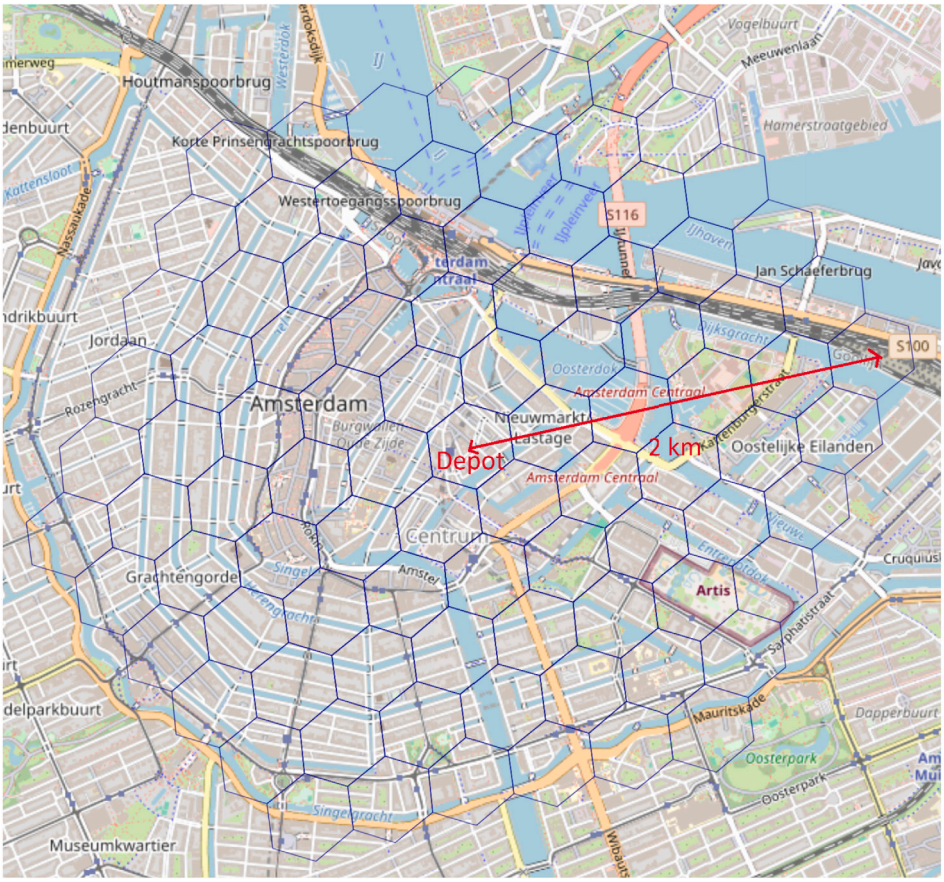


**Fig. 5.5.** Amsterdam inland waterway. MFI depot is located in the center and the radius of the test area is 2 km.

**Fig. 5.6.** (left) Electric waterborne vessels; (right) Canal of Amsterdam.
*Source:* (left) https://hykeelectricferries.com/urban-mobility-solutions; (right) taken by the authors.

**Table 5.15**
Indicators in the "Free" and "Base" configurations for Weekday and Weekend scenarios.

| Scn. | DP | | | Obj. (€) | | | Idle (min) | | |
|---|---|---|---|---|---|---|---|---|---|
| | Free | Base | **Diff.** | Free | Base | **Diff.** | Free | Base | **Diff.** |
| Weekday | 14 | 13 | 50% | 1219.75 | 1234.24 | 1.19% | 23.09 | 23.97 | 3.81% |
| Weekend | 19 | 19 | 26.30% | 1524.9 | 1532.28 | 0.48% | 24.64 | 24.91 | 1.10% |

**Table 5.16**
Sensitivity to rider shift length.

| Shift Len. | Obj. (€) | | | Bikes | | | Idle (min) | | |
|---|---|---|---|---|---|---|---|---|---|
| (h) | MFI | Bench. | Impr. | MFI | Bench. | Impr. | MFI | Bench. | Impr. |
| 2 | 1280.75 | 1648.05 | 22% | 23 | 27 | 15% | 20.22 | 36.89 | 45% |
| 3 | 1363.15 | 1646.29 | 17% | 28 | 31 | 10% | 23.78 | 36.67 | 35% |
| 4 | 1373.44 | 1656.13 | 17% | 31 | 31 | 0% | 24.11 | 37.11 | 35% |
| 5 | 1400.77 | 1653.67 | 15% | 31 | 31 | 0% | 25.33 | 37.00 | 32% |
| 6 | 1433.32 | 1656.83 | 13% | 31 | 35 | 11% | 26.89 | 37.00 | 27% |
| Ave. | 1370.29 | 1652.19 | 17% | 28.8 | 31 | 7% | 24.07 | 36.93 | 35% |

### *5.4.2. The day of the week*

Once set, the strategy configuration (MFI leasing, docking point locations, and the number of bikes) remains fixed for a long time. Historical data shows that customer orders vary throughout the week. Weekends typically have higher order volumes, while weekdays have lower volumes. This leads to slightly different rider shift patterns.

We define two scenarios: Weekday and Weekend. We consider 75% of the number of riders in the MFI-Base for the Weekday scenario and 125% for the Weekend scenario. Based on findings in Section 5.3.2, the required number of bikes is between 70% to 87% of the number of riders. The two scenarios maintain an identical spatial distribution of bike pickup and return demands to the MFI-Base, differing only in the number of demands in each zone. We consider two situations regarding the visitable docking points for the MFI in Weekday and Weekend scenarios: (1) "Base", where the MFI can only visit docking points that are selected in the MFI-Base; (2) "Free", where the MFI can visit all possible candidate docking points.

Table 5.15 presents the numbers of docking points, objective values, and the average idle time for Weekday and Weekend scenarios in the "Base" and "Free" situations. The "Diff." column under "DP" shows the percentage of the docking points that are different in "Free" compared to "Base". Under "Obj. (€)" and "Idle (min)", the "Diff." columns show the percentage difference between the indicator values in "Base" and "Free", calculated as $(Base - Free)/Free$. As can be seen in the table, while the number of visited docking points is very close between the "Base" and "Free" situations for both the Weekday and Weekend scenarios, the docking point locations change significantly: 50% of the docking points are different for Weekday and 26.3% for Weekend. However, there is a very slight increase in the objective values in the "Base" configuration compared to the "Free" for both the Weekday (1.19%) and Weekend (0.48%). Rider idle time also only increases very slightly, 3.81% for Weekday and 1.10% for Weekend. The results demonstrate the stability of the MFI strategy. We show that MFI-Base configurations, which are based on average daily rider numbers, remain effective for slightly changing rider shift patterns on weekdays and weekends.

### *5.4.3. Platform operation policies*

In this section, we investigate the impact of platform policies on the shift length and service range of riders. Changing these two factors may impose different pressures on the urgency of a zone requiring bikes or having bikes to return in certain periods. In the MFI-Base, the shift length of riders is 4 h and the service spatial range is the whole area.

**Sensitivity to rider shift length.** In this section, we use MFI-Base as a reference and vary the shift length as {2, 3, 4, 5, 6} h while keeping the service spatial range unchanged. Table 5.16 presents the objective value, the number of bikes, and the average rider idle time for MFI-Base and the stationary facility case (Column "Bench.") under different shift length. The columns "Impr" under each indicator report the percentage improvements after implementing the MFI strategy. The results show that longer service lengths lead to larger objective values and more bikes required, and riders spend more time on bike pickups and returns. This trend applies to both the MFI strategy and the stationary facility case. When comparing the MFI strategy and stationary facility case for the five shift lengths, the MFI strategy always has better system performance. On average, we see a decrease of 17% in the objective value, 7% in the required number of bikes, and 35% in the average rider idle time.

**Sensitivity of rider service spatial range.** In this analysis, we vary the radius of the rider service spatial range as {0, 2, 4, 6, 8, 10} zones while keeping the shift length as 4 h. A service range of 0 zone represents the case where riders start the first delivery and end the last one in the same zone. Table 5.17 shows the objective values and the average rider idle time for both the MFI and stationary facility case. The number of required bikes is always 31 for all cases. The results show the effect of changing the rider service range is small. When comparing the MFI strategy and the stationary facility case, we observe on average an improvement of 15% in the objective value and 32% in the average rider idle time.

**Table 5.17**
Sensitivity to rider service range.

| Range | Obj. (€) | | | Idle (min) | | |
|---|---|---|---|---|---|---|
| (zones) | MFI | Bench. | Impr. | MFI | Bench. | Impr. |
| 0 | 1409.80 | 1656.40 | 15% | 25.78 | 37.11 | 31% |
| 2 | 1388.20 | 1646.56 | 16% | 24.78 | 36.67 | 32% |
| 4 | 1389.31 | 1617.04 | 14% | 24.89 | 35.33 | 30% |
| 6 | 1363.06 | 1626.88 | 16% | 23.67 | 35.78 | 34% |
| 8 | 1385.47 | 1653.94 | 16% | 24.67 | 37.00 | 33% |
| 10 | 1373.44 | 1656.13 | 17% | 24.11 | 37.11 | 35% |
| Ave. | 1387.17 | 1640.16 | 15% | 24.76 | 36.38 | 32% |

## 6. Conclusion

This study investigates the potential of the MFI strategy for on-demand delivery services and proposes a mixed-integer optimization model to jointly optimize infrastructure investments and operational costs. The model is tractable for reasonably sized real-world instances and solvable within an acceptable time using a commercial solver. A case study in the Amsterdam inland waterway demonstrates the superiority and applicability of the MFI approach. Compared to the current stationary fleet inventory practice, our model reduces the total system cost by 17.07% and average rider idle time by 35.03%. Importantly, the optimized configuration that encompasses MFI leasing, docking point locations, and the number of shared bikes proves robust across typical variations in rider shift patterns between weekday and weekend scenarios.

While the results demonstrate the benefits of the MFI system through a case study in Amsterdam inland waterway, several avenues remain for future exploration. First, this study focuses on a specific operational area within Amsterdam's canal network as a proof-of-concept. Scaling the MFI system citywide involves operational considerations including local variation in canal access, customer demand density, and vessel navigability. For example, some areas are not accessible by water, or may not justify deployment due to lower order volume. These factors inform where and how MFIs are most effectively deployed, suggesting a modular design strategy that prioritizes high-demand, canal-accessible zones. To extend the framework to more diverse urban settings, future work may explore hybrid systems that combine MFIs with land-based alternatives such as electric trucks or cargo bikes, particularly in areas lacking sufficient water access. These systems would require additional modeling to address road-based uncertainties such as traffic conditions and delivery variability.

A second direction involves managing spatiotemporal fluctuations in delivery demand and rider availability. Although the current model operates at a strategic-tactical level with deterministic inputs, it can be extended to support adaptive planning under demand variability. This includes weekday–weekend shifts, seasonal changes, and event-driven surges. Robust optimization or scenario-based approaches could help maintain efficiency under foreseeable disruptions, without requiring full real-time responsiveness.

Finally, the model assumes an employment-based courier system using shared (e)bikes to reflect a shift toward better labor conditions. The framework can accommodate hybrid workforce models, including riders using personal vehicles compensated by shift or availability. Coordinating such systems, where centralized infrastructure intersects with decentralized rider behavior, presents a compelling direction for future research.

## CRediT authorship contribution statement

**C. Yang:** Writing – review & editing, Writing – original draft, Visualization, Validation, Software, Methodology, Investigation, Formal analysis, Data curation, Conceptualization. **M.Y. Maknoon:** Writing – review & editing, Writing – original draft, Validation, Supervision, Resources, Project administration, Methodology, Funding acquisition, Formal analysis, Data curation, Conceptualization. **H. Jiang:** Writing – review & editing, Supervision, Methodology, Conceptualization. **Sh. Sharif Azadeh:** Writing – review & editing, Writing – original draft, Visualization, Validation, Supervision, Project administration, Methodology, Investigation, Funding acquisition, Formal analysis, Conceptualization.

## Acknowledgments

This research was supported by JPI-ERANET and NWO under Grant C61A61, and their support is gratefully acknowledged.

## Appendix

### A.1. Constraints linearization

Constraints (23) in the arc-based formulation are nonlinear, which can be linearized as follows:

$$Q^{MFI}(1-x^{v}_{(z,t)(z',t')})I^{v}_{z't'} \geq I^{v}_{zt} + \sum_{(z'',t'')\in N^{R-}_{z,t}} y^{RM,v}_{(z'',t'')(z,t)} - \sum_{(z'',t'')\in N^{R+}_{z,t}} y^{PM,v}_{(z,t)(z'',t'')},$$

$$\forall v \in \mathcal{V}, \quad \forall (z,t) \in \mathcal{N}^{M}, \quad \forall (z',t') \in N^{M+}_{z,t}, \tag{63}$$

$$Q^{MFI}(x^{v}_{(z,t)(z',t')}-1)I^{v}_{z't'} \leq I^{v}_{zt} + \sum_{(z'',t'')\in N^{R-}_{z,t}} y^{RM,v}_{(z'',t'')(z,t)} - \sum_{(z'',t'')\in N^{R+}_{z,t}} y^{PM,v}_{(z,t)(z'',t'')},$$

$$\forall v \in \mathcal{V}, \quad \forall (z,t) \in \mathcal{N}^{M}, \quad \forall (z',t') \in N^{M+}_{z,t}. \tag{64}$$

Constraints (53) in the route-based formulation are non-linear, which can be linearized as:

$$Q^{MFI}(1-f^{l+1,k'}_{l,k}) + I^{l+1,k'}_{(z',t')} \geq I^{lk}_{(z,t)} + \sum_{(z'',t'')\in N^{R-}_{(z,t)}} y^{RM,lk}_{(z'',t'')(z,t)} - \sum_{(z'',t'')\in N^{R+}_{(z,t)}} y^{PM,l,k}_{(z,t),(z'',t'')},$$

$$\forall l \in L \setminus \{|L|\}, \quad \forall k \in K_l, \quad \forall k' \in K_{l+1}, \quad (z,t) = H^{lk}(-1), \quad (z',t') = H^{l+1,k'}(1), \tag{65}$$

$$Q^{MFI}(f^{l+1,k'}_{l,k}-1) + I^{l+1,k'}_{(z',t')} \leq I^{lk}_{(z,t)} + \sum_{(z'',t'')\in N^{R-}_{(z,t)}} y^{RM,lk}_{(z'',t'')(z,t)} - \sum_{(z'',t'')\in N^{R+}_{(z,t)}} y^{PM,l,k}_{(z,t),(z'',t'')},$$

$$\forall l \in L \setminus \{|L|\}, \quad \forall k \in K_l, \quad \forall k' \in K_{l+1}, \quad (z,t) = H^{lk}(-1), \quad (z',t') = H^{l+1,k'}(1). \tag{66}$$

### A.2. Variable reduction

The upper bounds of all integer variables can be determined beforehand. Based on specific inputs, the demands for bike pickup and return occurring at node $(z,t)$ might be 0. This means that the upper bounds of the variables associated with satisfying these bike pickups and returns are 0. These variables can be removed from the model before solving.

The following variables associated with satisfying bike pickups and returns occurring at $(z,t)$ through MFIs can be reduced if the input shows no bike pickups and returns there:

- $\sum_{v\in\mathcal{V}} \sum_{(z'',t'')\in N^{R-}_{z,t}\cap\mathcal{N}^{M}} y^{PM,v}_{(z'',t'')(z,t)} = 0 \quad \text{if } d_{zt} = 0.$
- $\sum_{l\in L} \sum_{k\in K_l} \sum_{(z'',t'')\in N^{R-}_{z,t}\cap H^{lk}} y^{PM,lk}_{(z'',t'')(z,t)} = 0 \quad \text{if } d_{zt} = 0.$
- $\sum_{v\in\mathcal{V}} \sum_{(z'',t'')\in N^{R+}_{z,t}\cap\mathcal{N}^{M}} y^{RM,v}_{(z,t)(z'',t'')} = 0 \quad \text{if } r_{zt} = 0.$
- $\sum_{l\in L} \sum_{k\in K_l} \sum_{(z'',t'')\in N^{R+}_{z,t}\cap H^{lk}} y^{RM,lk}_{(z,t)(z'',t'')} = 0 \quad \text{if } r_{zt} = 0.$

Similarly, variables associated with docking points can be removed if the inputs show there are no bike pickups and returns at $(z,t)$:

- $\sum_{(z'',t'')\in N^{R-}_{z,t}\cap\mathcal{N}^{M}} y^{PD}_{(z'',t'')(z,t)} \quad \text{if } d_{zt} = 0.$
- $\sum_{(z'',t'')\in N^{R+}_{(z,t)}\cap\mathcal{N}^{M}} y^{RD}_{(z,t),(z'',t'')} = 0 \quad \text{if } r_{zt} = 0.$

Also, variables related to self-fulfillment when inputs show no bike pickups and returns at $(z,t)$:

- $\sum_{(z'',t'')\in N^{R-}_{z,t}} y^{SF}_{(z'',t'')(z,t)} = 0 \quad \text{if } d_{zt} = 0.$
- $\sum_{(z'',t'')\in N^{R+}_{z,t}} y^{SF}_{(z,t)(z'',t'')} = 0 \quad \text{if } r_{zt} = 0.$

## Data availability

Data will be made available on request.

## References

Alarcon-Gerbier, E., Buscher, U., 2020. Minimizing movements in location problems with mobile recycling units. In: Computational Logistics: 11th International Conference, ICCL 2020, Enschede, the Netherlands, September 28–30, 2020, Proceedings 11. Springer, pp. 396–411.

Alarcon-Gerbier, E., Buscher, U., 2022. Modular and mobile facility location problems: A systematic review. Comput. Ind. Eng. 173, 108734.

Ataç, S., Obrenović, N., Bierlaire, M., 2021. Vehicle sharing systems: A review and a holistic management framework. EURO J. Transp. Logist. 10, 100033.

Auad-Perez, R., Van Hentenryck, P., 2022. Ridesharing and fleet sizing for on-demand multimodal transit systems. Transp. Res. Part C: Emerg. Technol. 138, 103594.

Bahrami, S., Nourinejad, M., Yin, Y., Wang, H., 2023. The three-sided market of on-demand delivery. Transp. Res. Part E: Logist. Transp. Rev. 179, 103313.

Bayraktar, O.B., Günneç, D., Salman, F.S., Yücel, E., 2022. Relief aid provision to en route refugees: Multi-period mobile facility location with mobile demand. European J. Oper. Res. 301 (2), 708–725.
Becker, T., Lier, S., Werners, B., 2019. Value of modular production concepts in future chemical industry production networks. European J. Oper. Res. 276 (3), 957–970.
Benjaafar, S., Wu, S., Liu, H., Gunnarsson, E.B., 2022. Dimensioning on-demand vehicle sharing systems. Manag. Sci. 68 (2), 1218–1232.
Büsing, C., Comis, M., Schmidt, E., Streicher, M., 2021. Robust strategic planning for mobile medical units with steerable and unsteerable demands. European J. Oper. Res. 295 (1), 34–50.
Calogiuri, T., Ghiani, G., Guerriero, E., Manni, E., 2021. The multi-period p-center problem with time-dependent travel times. Comput. Oper. Res. 136, 105487.
CCNR, 2022. Inland Waterway Transport Embedded in Urban Logistics. CCNR, https://inland-navigation-market.org/chapitre/{{2}}-inland-waterway-transport-embedded-in-urban-logistics/lang=en. Accessed: 2024.
Çelebi, D., Yörüsün, A., Işık, H., 2018. Bicycle sharing system design with capacity allocations. Transp. Res. Part B: Methodol. 114, 86–98.
Chakraborty, J., Pandit, D., Chan, F., Xia, J., 2021. A review of ride-matching strategies for ridesourcing and other similar services. Transp. Rev. 41 (5), 578–599.
de Vries, H., Van de Klundert, J., Wagelmans, A.P., 2020. The roadside healthcare facility location problem a managerial network design challenge. Prod. Oper. Manage. 29 (5), 1165–1187.
Demaine, E.D., Hajiaghayi, M., Mahini, H., Sayedi-Roshkhar, A.S., Oveisgharan, S., Zadimoghaddam, M., 2009. Minimizing movement. ACM Trans. Algorithms (TALG) 5 (3), 1–30.
DeMaio, P., 2009. Bike-sharing: History, impacts, models of provision, and future. J. Public Transp. 12 (4), 41–56.
Du, M., Cheng, L., Li, X., Tang, F., 2020. Static rebalancing optimization with considering the collection of malfunctioning bikes in free-floating bike sharing system. Transp. Res. Part E: Logist. Transp. Rev. 141, 102012.
Fan, Q., van Essen, J.T., Correia, G.H., 2023. Optimising fleet sizing and management of shared automated vehicle (SAV) services: A mixed-integer programming approach integrating endogenous demand, congestion effects, and accept/reject mechanism impacts. Transp. Res. Part C: Emerg. Technol. 157, 104398.
Farahani, R.Z., Hekmatfar, M., 2009. Facility location: concepts, models, algorithms and case studies.
Friggstad, Z., Salavatipour, M.R., 2011. Minimizing movement in mobile facility location problems. ACM Trans. Algorithms (TALG) 7 (3), 1–22.
Güden, H., Süral, H., 2014. Locating mobile facilities in railway construction management. Omega 45, 71–79.
Guo, Z., Hao, M., Yu, B., Yao, B., 2021. Robust minimum fleet problem for autonomous and human-driven vehicles in on-demand ride services considering mixed operation zones. Transp. Res. Part C: Emerg. Technol. 132, 103390.
Hu, L., Liu, Y., 2016. Joint design of parking capacities and fleet size for one-way station-based carsharing systems with road congestion constraints. Transp. Res. Part B: Methodol. 93, 268–299.
Illgen, S., Höck, M., 2019. Literature review of the vehicle relocation problem in one-way car sharing networks. Transp. Res. Part B: Methodol. 120, 193–204.
Kruse, J., Kang, D.H., Monsreal, M., et al., 2022. Inland waterway travel time prediction: November 2020 to march 2022.
Lei, C., Lin, W.-H., Miao, L., 2014. A stochastic emergency vehicle redeployment model for an effective response to traffic incidents. IEEE Trans. Intell. Transp. Syst. 16 (2), 898–909.
Mandal, M.P., Santini, A., Archetti, C., 2025. Tactical workforce sizing and scheduling decisions for last-mile delivery. European J. Oper. Res. 323 (1), 153–169.
Monteiro, C.M., Machado, C.A.S., de Oliveira Lage, M., Berssaneti, F.T., Davis, Jr., C.A., Quintanilha, J.A., 2021. Optimization of carsharing fleet size to maximize the number of clients served. Comput. Environ. Urban Syst. 87, 101623.
Narayan, J., Cats, O., van Oort, N., Hoogendoorn, S.P., 2021. Fleet size determination for a mixed private and pooled on-demand system with elastic demand. Transp. Transp. Sci. 17 (4), 897–920.
Narayanan, S., Chaniotakis, E., Antoniou, C., 2020. Shared autonomous vehicle services: A comprehensive review. Transp. Res. Part C: Emerg. Technol. 111, 255–293.
Parr, T., 2018. Boat-bike: DHL's multimodal Amsterdam logistics chain. URL: https://www.rippl.bike/en/rippl-36-boat-bike-dhls-multimodal-amsterdam-logistics-chain/.
Pashapour, A., Günneç, D., Salman, F.S., Yücel, E., 2024. Capacitated mobile facility location problem with mobile demand: Efficient relief aid provision to en route refugees. Omega 103138.
Qu, B., Mao, L., Xu, Z., Feng, J., Wang, X., 2021. How many vehicles do we need? Fleet sizing for shared autonomous vehicles with ridesharing. IEEE Trans. Intell. Transp. Syst. 23 (9), 14594–14607.
Raghavan, S., Sahin, M., Salman, F.S., 2019. The capacitated mobile facility location problem. European J. Oper. Res. 277 (2), 507–520.
Salman, F.S., Yücel, E., Kayı, İ., Turper-Alışık, S., Coşkun, A., 2021. Modeling mobile health service delivery to Syrian migrant farm workers using call record data. Socio Econ. Plan. Sci. 77, 101005.
Schuijbroek, J., Hampshire, R.C., Van Hoeve, W.-J., 2017. Inventory rebalancing and vehicle routing in bike sharing systems. European J. Oper. Res. 257 (3), 992–1004.
Shehadeh, K.S., 2023. Distributionally robust optimization approaches for a stochastic mobile facility fleet sizing, routing, and scheduling problem. Transp. Sci. 57 (1), 197–229.
Shehadeh, K.S., Wang, H., Zhang, P., 2021. Fleet sizing and allocation for on-demand last-mile transportation systems. Transp. Res. Part C: Emerg. Technol. 132, 103387.
Vazifeh, M.M., Santi, P., Resta, G., Strogatz, S.H., Ratti, C., 2018. Addressing the minimum fleet problem in on-demand urban mobility. Nat. 557 (7706), 534–538.
Yang, J., Levin, M.W., Hu, L., Li, H., Jiang, Y., 2023. Fleet sizing and charging infrastructure design for electric autonomous mobility-on-demand systems with endogenous congestion and limited link space. Transp. Res. Part C: Emerg. Technol. 152, 104172.
Yücel, E., Salman, F.S., Bozkaya, B., Gökalp, C., 2020. A data-driven optimization framework for routing mobile medical facilities. Ann. Oper. Res. 291, 1077–1102.